JVI Accepted Manuscript Posted Online 26 July 2017
J. Virol. doi:10.1128/JVI.00279-17

Full title: Role of Viral Hemorrhagic Septicemia Virus Matrix (M) Protein in Suppressing Host Transcription

Authors: Qi Ke [a1]*, Wade Weaver [a]*, Adam Pore [a], Bartolomeo Gorgoglione [a], Julia Halo Wildschutte [a2], Peng Xiao [b3], Brian S. Shepherd [c], Allyn Spear [c], Krishnamurthy Malathi [a], Carol A. Stepien [d], Vikram N. Vakharia [b], Douglas W. Leaman [a]†

Affiliations: Department of Biological Sciences, The University of Toledo, Toledo, Ohio, 43606 USA[a]; Institute of Marine and Environmental Technology, University of Maryland Baltimore County, Baltimore, Maryland 21202 USA[b]; USDA/ARS/School of Freshwater Sciences/University of Wisconsin-Milwaukee, 600 E. Greenfield Ave., Milwaukee, WI 53204 USA[c]; NOAA Pacific Marine Environmental Laboratory (PMEL), 7600 Sand Point Way NE, Seattle, WA 98115 USA[d]

† Corresponding author phone: 1-937-775-3180; Fax: 1-937-775-4678; Email: douglas.leaman@wright.edu; Address: Wright State University, 4035 Colonel Glenn Hwy., Suite 300, Beavercreek, OH 45431, USA

*Q.K and W.W. contributed equally to this work

Running Title: VHSV M in host immune suppression

[1] Present address: The University of North Carolina at Chapel Hill, 6111 Marsico Hall, 125 Mason Farm Road, CB #7290, Chapel Hill, NC 27599 USA
[2] Present address: Bowling Green State University, 521A Life Sciences Building, Bowling Green, OH 43403 USA
[3] Present Address: Institute of Oceanology, Chinese Academy of Sciences, Qingdao 26607, P.R. CHINA

Abstract

Viral Hemorrhagic Septicemia virus (VHSV) is a pathogenic fish rhabdovirus found in discrete locales throughout the northern hemisphere. VHSV infection of fish cells leads to upregulation of the host's virus detection response, but the virus quickly suppresses interferon (IFN) production and antiviral genes expression. By systematically screening each of the six VHSV structural and nonstructural genes, we have identified matrix protein (M) as its most potent anti-host protein. VHSV-IVb M alone suppressed mitochondrial antiviral signaling protein (MAVS) and type I IFN-induced gene expression in a dose-dependent manner. M also suppressed the constitutively active SV40 promoter and globally decreased cellular RNA levels. Chromatin immunoprecipitation (ChIP) studies illustrated that M inhibited RNA polymerase II (RNAP II) recruitment to gene promoters, and decreased RNAP II CTD Ser2 phosphorylation during VHSV infection. However, transcription directed by RNAP I-III was suppressed by M. To identify regions of functional importance, M proteins from a variety of VHSV strains were tested in cell-based transcriptional inhibition assays. M protein of a particular VHSV-Ia strain, F1, was significantly less potent than -IVb M at inhibiting SV40/luc expression, yet differed by just four amino acids. Mutation of D62 to alanine alone, or in combination with an E181 to alanine mutation (D62A/E181A), dramatically reduced the ability of -IVb M to suppress host transcription. Introducing either M D62A or D62A/E181A mutations into VHSV-IVb via reverse genetics resulted in viruses that replicated efficiently but exhibited less cytotoxicity and reduced anti-transcriptional activities, implicating M as a primary regulator of cytopathicity and host transcriptional suppression.

Importance: Viruses must suppress host antiviral responses to replicate and spread between hosts. In these studies, we identified the matrix protein of the deadly fish Novirhabdovirus, VHSV, as a critical mediator of host suppression during infection. Our studies indicated that M alone could block cellular gene expression at very low expression levels. We identified several subtle mutations in M that were less potent at suppressing host transcription. When these mutations were engineered

50 back into recombinant viruses, the resulting viruses replicated well but elicited less toxicity in
51 infected cells and activated host innate immune responses more robustly. These data demonstrated
52 that VHSV M plays an important role in mediating both virus-induced cell toxicity and viral
53 replication. Our data suggest that its roles in these two processes can be separated to design
54 effective attenuated viruses for vaccine candidates.
55

56 **Introduction**

57 Higher eukaryotes have evolved complex innate immune systems that serve as the first line of
58 defense against pathogens like bacteria, fungi and viruses. Host cells detect conserved pathogen-
59 associated molecular patterns (PAMPs) via germline-encoded pattern recognition receptors (PRRs)
60 (1), which, once activated, initiate signaling cascades to produce anti-pathogenic factors such as
61 type I interferons (IFNs) and other pro-inflammatory cytokines (2). The retinoic acid-inducible
62 gene 1 (RIG-I)-like helicases (RLHs) including RIG-I, melanoma differentiation associated factor 5
63 (MDA5) and laboratory of genetics and physiology 2 (LGP2) are cytoplasmic PRRs, expressed in
64 both immune and nonimmune cells, which are essential for detection of intracellular RNA
65 products, primarily of viral origin (3). Upon activation, both RIG-I and MDA5 recruit and activate
66 MAVS (mitochondrial antiviral signaling protein; also called IPS-1/Cardif/VISA) (4), leading to
67 activation of downstream signaling molecules and induction of type I IFNs and other
68 dsRNA/virally regulated genes (5-7). Secreted IFNs binds to the cognate type I IFN receptor
69 (IFNAR) complex and activate signal transducer and activator of transcription (STAT)-dependent
70 signaling cascades that lead to transcription of IFN-stimulated genes (ISGs) (8). ISG proteins
71 impact a variety of cellular functions, including transcriptional and translational regulation, pro-
72 and anti-apoptotic processes, cell signaling, etc., and work together to establish an antiviral state
73 (9). Perturbation of the viral detection or IFN response pathways leads to enhanced sensitivity to
74 most viruses.

75 The IFN system is highly conserved from mammals down to bony fish (10-12). Teleost

76 IFNs are similar to mammalian type I IFNs based on coding sequences and crystalline structure
77 analysis, although the fish genes differ from their mammalian counterparts by the inclusion of
78 introns (13-15). All of the critical signaling molecules in the viral detection and IFN response
79 pathways have been cloned from multiple fish species, including RLHs, Janus kinase (JAK) and
80 STAT signaling molecules and a number of traditional ISGs, such as Mx (13,16-18). These studies
81 suggest that the innate antiviral pathways and proteins in teleost fish share many regulatory features
82 in common with their mammalian orthologues.

83 Viral Hemorrhagic Septicemia virus (VHSV) causes severe disease and mortality among
84 more than 90 marine and freshwater fish species worldwide (19,20). VHSV is a bullet-shaped,
85 enveloped, non-segmented negative sense single-stranded RNA virus in the *Novirhabdovirus* genus
86 of the *Rhabdoviridae* family (20). Its 11-kb viral genome contains 6 genes encoding (in order from
87 3'-to-5'): nucleoprotein (N), phosphoprotein (P), matrix protein (M), glycoprotein (G), NonVirion
88 protein (NV), and RNA-dependent RNA polymerase (L) (21,22). Replication occurs entirely in the
89 cytoplasm using a combination of virally encoded and host-derived factors. VHSV isolates are
90 classified in four genotypes (designated I to IV) based on phylogenetic analysis (23). Each group is
91 endemic to specific geographic regions, with freshwater strains included in genotypes I and IV, and
92 each appears to infect regional fish species (24). Genotype I is further divided into five sublineages
93 (Ia-Ie), with the -Ia strain responsible for most outbreaks in European freshwater rainbow trout
94 farms (20,23,25,26). Genotype IV viruses are further divided into three sublineages – -IVa, -IVb
95 and -IVc (24). In 2005, VHSV-IVb was first isolated from muskellunge (*Esox masquinongy*) from
96 Lake Ontario and subsequently found in an archived sample from Lake St. Clair dating back to
97 2003 (isolate MI03GL) (27). VHSV-IVb caused massive die-offs among many freshwater species
98 during the next decade and continues to pose a potential threat to both fish farming and the sport
99 fishing industry in the Great Lakes watershed (28-30). VHSV-IVb has been isolated from at least
100 31 fish species including muskellunge, yellow perch and walleye (28) and has been detected in all
101 five of the Laurentian Great Lakes (31,32). However, unlike the European -Ia sublineage, -IVb has

102 low pathogenicity for rainbow trout (33). Despite intensive management and surveillance, VHSV is
103 still detectable among many asymptomatic fish in the Great Lakes region (34).

104 As with other viruses, VHSV must suppress or evade components of the host antiviral
105 responses in order to propagate. Studies have suggested that NV protein from the -IVb sublineage
106 suppressed apoptosis (35) and from the -Ia sublineage suppressed innate immune responses (36,37).
107 M protein has been implicated in cellular apoptosis and transcriptional suppression in the related
108 fish Novirhabdovirus Infectious Hematopoietic Necrosis virus (IHNV) (38). Several M variants
109 have been found for VHSV-IVb (39), but little else is known about VHSV-IVb anti-host processes.

110 We have undertaken a systematic study of VHSV-IVb proteins to identify which might
111 contribute to anti-host activities. VHSV infection of fish cells led to activation of the virus
112 detection system, but the virus quickly suppressed IFN production and antiviral gene expression.
113 By screening each of the six viral structural and nonstructural genes, we have identified M protein
114 as the most potent anti-host protein expressed by VHSV-IVb. Comparative studies with M isolated
115 from other VHSV strains or other fish Novirhabdoviruses identified mutations that reduced anti-
116 transcriptional function. In particular, point mutations of the aspartic acid at residue 62 (D62G or
117 D62A) and/or the glutamic acid residue at position 181 (E181A) had combinatorial effects on M
118 anti-transcriptional potential (D62A/E181A). When reverse engineered into recombinant viruses
119 the M single and double mutations led to reduced anti-host activities that altered viral cytopathicity
120 and antiviral genes expression. These data suggested that VHSV M is a pivotal component of the
121 VHSV suppression of host antiviral responses, and that targeting M for mutation has the potential
122 to undermine this anti-host function without destroying the viral replication function of M.

123

124 **Results**

125 **VHSV inhibits IFN antiviral signaling**

126 To study the effect of VHSV infection on host innate immune detection and IFN production, EPC
127 cells were treated with or without IFN (EPC-derived type I IFN) either 24 h prior to, or 16 or 24 h

128 post infection (h.p.i). VHSV-IVb was used at MOI 1 and cellular cytopathic effects (CPE) were
129 assessed at 72 h.p.i. (Fig. 1A). Infection resulted in significant CPE, which was completely
130 prevented by IFN pretreatment (Fig. 1A). In contrast, IFN added 16 or 24 h.p.i. was ineffective at
131 blocking viral CPE, despite the fact that no cell death was observed at the time of IFN addition
132 (Fig. 1A). These data suggest that upon infection, VHSV produces a factor or factors that are
133 capable of shutting down host IFN-mediated antiviral responses. To further dissect the interplay
134 between viral infection and cellular IFN production, EPC cells were transiently transfected with a
135 luciferase reporter under the control of the IFN-responsive IFITM1 promoter. Cells were left
136 uninfected or infected with VHSV for 24 or 48 h and untreated or treated with IFN for the final 6 h
137 prior to the luciferase assay (Fig. 1B). As expected, viral infection alone led to a 6- to 10-fold
138 increase in IFN-induced transcription from the IFITM1 promoter as compared to uninfected cells
139 (Fig. 1B). However, this induction was far less than that observed with IFN treatment alone. More
140 importantly, viral infection suppressed responsiveness to exogenous by 80-90% as compared to
141 IFN treatment alone (Fig. 1B). These data provide evidence that VHSV is capable of inhibiting IFN
142 production in host cells, and/or blocking their response to IFN.
143
144 **VHSV-IVb M inhibits host gene expression**
145 To identify viral proteins involved in the inhibitory effect of VHSV on host IFN responsiveness,
146 each of the six VHSV structural and nonstructural genes was cloned into pcDNA3.1 expression
147 plasmid and then co-transfected along with IFITM1/luc and EPC-derived MAVS in EPC cells.
148 Ectopic MAVS expression was sufficient to induce endogenous IFN expression and release, which
149 fed back on the cells to activate the IFITM1 promoter. Although several of the viral genes had
150 subtle effects on IFITM1 induction, only the pcDNA3.1 M plasmid (pCD-M) potently decreased
151 IFITM1 promoter activation (Fig. 2A). Conversely, NV was able to upregulate luciferase activity
152 from the IFITM1 promoter. Although each of the Myc tagged VHSV genes was clearly expressed
153 in the EPC cells, VHSV M was consistently reduced in expression due to feedback inhibition of the

154 plasmid promoter (Fig. 2B). To determine whether the impact of M was downstream of IFN
155 expression, cells were transiently transfected with pCD-M and IFITM1/luc and then treated with
156 IFN for 24 h. VHSV-IVb M potently inhibited luciferase expression with an IC50 less than 0.5 ng
157 plasmid/5×10^5 cells (Fig. 2C). For analysis of pathways upstream of IFN, EPC cells were co-
158 transfected with MAVS, pCD-M and an IFN promoter-luciferase reporter plasmid (IFN/luc) for 24
159 h. M again potently blocked induction of luciferase activity in a dose-dependent manner (Fig. 2D),
160 with 80% inhibition observed at concentrations of just 0.5 ng of pCD-M/5×10^5 cells. The potent
161 inhibition of both IFN and ISG transcriptional induction suggested that M either selectively
162 targeted components of both pathways, or that it was a general inhibitor of gene transcription or
163 translation. To test this, pCD-M was co-transfected with an unrelated, constitutively active SV40
164 promoter-luciferase reporter (SV40/luc). VHSV M again potently inhibited SV40 promoter activity
165 in a dose-dependent manner (Fig. 2E), suggesting that M inhibits a general step in cellular protein
166 expression – either transcription or translation. To clarify whether M functioned as a transcriptional
167 or translational inhibitor, cells again were co-transfected with pCD-M and SV40/luc plasmids and
168 luciferase mRNA was quantified via RT-qPCR (Fig. 3A). M co-expression induced a dose-
169 dependent decrease in luciferase mRNA expression, strongly implicating an impact on cellular
170 RNA transcription or half-life. Since the impact of M on luciferase mRNA was not as potent as that
171 observed when measuring luciferase activity (Fig. 3A compared to 2E), we reasoned that M either
172 exhibited secondary effects on mRNA translation or that luciferase mRNA expression begins in
173 cells before the co-transfected M can elicit an inhibitory effect. Thus, to measure the impact of M
174 on transcriptional initiation instead of pre-existing steady mRNA levels, we co-transfected pCD-M
175 with a regulatable plasmid encoding a mouse SEAP (secreted embryonic alkaline phosphatase)
176 reporter gene under the transcriptional control of a tetracycline responsive element (Tet). After 24
177 h, transfected cells were left unstimulated or were treated with doxycycline for 24 h prior to RNA
178 extraction and RT-qPCR analysis of SEAP mRNA levels. Under these conditions, SEAP mRNA
179 induction was completely inhibited by M co-expression (Fig. 3B). Taken together, these data

180 suggest that the primary anti-host effect of VHSV-IVb M is to inhibit host cellular transcription
181 during viral infection.
182
183 **VHSV M blocks nascent cellular RNA synthesis**
184 Previous studies focused on the anti-host role of Vesicular Stomatitis Virus (VSV) M protein and
185 demonstrated direct inhibition of host transcription (40). To determine if VHSV M behaved
186 similarly, we utilized an analog of uracil, 5-ethynyl uridine (EU), to study active (nascent) cellular
187 RNA synthesis. EU contains an alkyne that can react with an azide-modified fluorophore to give
188 fluorescent signal (41,42). EPC cells were left untreated, treated with α-Amanitin (1 μg/ml),
189 Actinomycin D (1 μg/ml) or infected with VHSV-IVb (MOI 1) for 24 h then pulsed with EU for 2
190 h, labeled with the Click-iT reagent and imaged. Untreated, labeled cells showed nuclear RNA
191 staining with strong puncta representing rRNA synthesis. α-Amanitin, which inhibits
192 predominantly RNAP II-mediated transcription at the dose used (43), showed strongly suppressed
193 nuclear labeling, albeit with residual rRNA nucleolar staining (Fig. 4A). In contrast, Actinomycin
194 D, which inhibits RNAP I, II and III, and thus served as a control for complete transcriptional
195 inhibition, suppressed all RNA synthesis in treated cells. EU staining in VHSV infected cells
196 mimicked the pattern observed with α-Amanitin treatment, although residual nucleolar staining in
197 VHSV infected cells was demonstrably less than in α-Amanitin treated cells (Fig. 4A). These data
198 suggested that VHSV-IVb potently inhibited activity of all three RNA polymerases to varying
199 degrees. To assess a direct role for M in the observed virus-dependent inhibition of host
200 transcription, we co-transfected pCD-M with a CMV-regulated green fluorescent protein (GFP)
201 plasmid (CMV/GFP, used as a marker of transfection) into EPC cells for 24 h and then labeled cells
202 with 5-EU. M transfected cells exhibited decreased nascent cellular RNA staining as compared to
203 GFP-only transfected control cells (Fig. 4B). The nascent cellular RNA reduction mirrored that
204 observed upon viral infection, implicating M as a contributing viral protein.
205 To more precisely define which transcriptional responses might be inhibited by M, we tested

206 VHSV M inhibitory potency on RNAP I, II and III promoters in cell-based luciferase assays. The
207 SV40/luc reporter was used again as an indicator of RNAP II-dependent transcription. A human
208 U6/luc reporter was employed to monitor RNAP III-dependent transcription, and a rainbow trout
209 rRNA intergenic sequence region (ITS-1/luc) reporter was used to assess RNAP I-dependent
210 transcription. Luciferase mRNA levels were measured by RT-qPCR since RNAP I and III do not
211 promote efficient protein production. VHSV-IVb M inhibited the activity of all three promoters,
212 but the RNAP II-regulated promoter appeared to be slightly more sensitive to the inhibitory effects
213 of M than were the RNAP I and RNAP III promoters (Fig. 4C,D). Previous studies had implicated
214 VSV M in suppression of all three RNA polymerases with different efficacy (44), and our studies
215 suggest that VHSV-IVb M is similarly effective in blocking RNAP I-III dependent transcription.

216 Subcellular localization studies using the myc/his tagged M revealed both nuclear and
217 cytoplasmic localization, consistent with a proposed role both in viral packaging and host
218 transcriptional suppression (Fig. 5A, B). In addition to direct inhibition of cellular transcription,
219 previous studies on VSV M protein had implicated a role in blocking nuclear export of mRNAs
220 (45-48). To determine whether VHSV infection alters the subcellular distribution of cellular
221 mRNAs, EPC cells (5×10^6) either were left uninfected or were infected with VHSV-IVb strain
222 (MOI 1) for 24 h. Cells were separately treated with Leptomycin B (LMB) for 3 h as a control for
223 nuclear export inhibition. After treatment or infection, cells pellets were spiked with 1×10^5 human
224 (HEK 293) cells to serve as an internal control. The cell mixtures then were separated into nuclear
225 and cytoplasmic fractions and RNA isolated from each. RT-qPCR then was performed to assess the
226 subcellular distribution of fish ß-actin mRNA in the uninfected, infected or LMB treated cells. To
227 control for variability in fractionation fidelity or RNA extraction efficiency, human GAPDH
228 mRNA was quantified in parallel and used to normalize the β-actin mRNA values. Since the human
229 cells had not been infected or treated with LMB, the human GAPDH mRNA distribution in the
230 spiked HEK 293 cells was expected to be identical in each sample, and the human primers were
231 designed and validated not to cross-react with EPC GAPDH cDNA (data not shown). VHSV

232 infection resulted in a decrease in overall β-actin mRNA levels, but had only a moderate impact on
233 the nuclear to cytoplasmic ratio as compared to uninfected cells (Fig. 5C, D). In contrast, LMB
234 altered dramatically the proportion of mRNA in the nucleus relative to the cytoplasm (Fig. 5C, D).
235 From these data, we cannot rule out a minor role for M in altering mRNA subcellular localization,
236 but its primary anti-host effect appears to be the inhibition of nascent transcription.
237

238 **VHSV-IVb M protein disrupted RNAP II activity and recruitment**

239 To gain further insight into the mechanism by which M inhibits host transcription, we used
240 chromatin immunoprecipitation (ChIP) to assess the impact of VHSV-IVb M on recruitment of
241 RNAP II to a core promoter sequence. EPC cells were co-transfected with Tet-mSEAP (as in Fig.
242 3) and pCD-M for 24 h and then left untreated or treated with doxycycline for 4 h, after which ChIP
243 analyses were performed using an RNAP II antibody and primers representing TATA-proximal
244 primers. RNAP II was constitutively bound to the promoter, but binding was augmented upon
245 doxycycline treatment (Fig. 6A). With pCD-M co-transfection, both uninduced and induced RNAP
246 II binding was significantly decreased (Fig. 6A).

247 The C-terminal domain (CTD) of RPB1, the largest RNAP II subunit, consists of 25 to 52
248 tandem copies of a conserved YSPTSPS heptapeptide repeat (49). During transcript elongation, the
249 RNAP II CTD is phosphorylated, predominantly at Ser2 and Ser5 residues, and these modifications
250 indicate different phases of transcription and RNAP II activity (50-52). Early in the transition from
251 preinitiation to elongation, the CTD is phosphorylated primarily on Ser5 residues. During
252 elongation, phosphorylation occurs mainly on Ser2 residues to generate elongation-proficient
253 RNAP II, and by the 3′ end of the gene CTD phosphorylation is dominated by Ser2 residues. To
254 address which phase of transcription was impacted, we infected EPC cells with VHSV for 0-72 h
255 and assessed total and Ser2 phosphorylated RNAP II levels by immunoblotting. Ser2
256 phosphorylation decreased during the course of a VHSV infection and, interestingly, total RNAP II
257 exhibited a mobility shift from a slower migrating form to a more rapidly migrating band over the

258 course of the infection (Fig. 6B). Together, these data suggest that VHSV-IVb M protein inhibits
259 host cellular transcription to suppress host immune responses by disrupting RNAP II recruitment
260 and subsequent phosphorylation, thereby preventing transcriptional initiation and elongation.
261
262 **Comparative studies on fish rhabdoviral M proteins**
263 Many of the observed VHSV-IVb M effects on EPC cells mirrored those observed previously with
264 VSV M in mammalian cells (44). To extend our studies beyond IVb M, we assessed the effects of
265 M proteins from various VHSV sublineages, as well as M proteins from the related fish
266 rhabdoviruses Infectious Hematopoietic Necrosis virus (IHNV), Spring Viremia of Carp virus
267 (SVCV) and Snakehead Rhabdovirus (SHRV), in cell-based luciferase inhibition assays. Each M
268 gene was cloned into pcDNA3.1 and co-transfected with SV40/luc into EPC cells for 24 h, after
269 which time luciferase assays were performed. Like VHSV-IVb M, all rhabdoviral M proteins
270 inhibited luciferase expression to varying degrees, although M from SVCV and SHRV exhibited
271 less activity than those in VHSV and IHNV (Fig. 7A) and, in the case of SHRV, required higher
272 plasmid concentrations to exhibit inhibition in these cells (data not shown). Subsequently western
273 blotting analysis was used to confirm the expression of rhabdoviral M proteins (Fig. 7B). Although
274 all VHSV strain M proteins had similar activities to -IVb M, one important exception was a variant
275 M protein from VHSV-Ia strain (F1), which exhibited significantly less inhibition than M from the
276 -IVb strain when monitoring nascent RNA synthesis (Fig. 7C). This -Ia M variant differed from -
277 IVb M at only four amino acid positions (T9I, D62G, E181A and V198A). In order to determine
278 which of these changes impacted anti-transcriptional activity, we mutated these same residues in
279 various combinations within the VHSV-IVb M background. The two residues that impacted
280 activity the most were at 62 and 181. Reverse mutations (G62D, G62D and A181E) within the -Ia
281 (F1) backbone rescued the anti-transcriptional efficacy of M (data not shown), whereas -IVb M
282 mutated singly at position 62 or doubly at 62 and 181 (D62A, D62A and E181A) each experienced
283 about 90% reduction in efficacy (Fig. 8A,B). The effect of these mutations on global host

284 transcription was also assessed by measuring RNAP II phosphorylation. For these studies, EPC
285 cells were transfected with either WT or mutant M Myc-His encoding plasmids for 48 h, and
286 RNAP II C-terminal domain (CTD) serine-2 phosphorylation was assessed using a RNAP II
287 phosphoserine-2 specific antibody (αRNAP II-Ps2) in immunofluorescence experiments. Cells
288 expressing either of the VHSV M constructs were visualized using an anti-Myc monoclonal
289 antibody (mAb) and FITC conjugated goat-anti-mouse antibody. These studies showed cells
290 expressing the mutant M proteins exhibited more prominent RNAP II-Ps2 staining as compared to
291 the RNAP II-Ps2 staining seen in WT M expressing cells (Fig. 8C). These data suggested that the
292 D62A or D62A/E181A M mutants were not as effective as WT M at inhibiting RNAP II
293 phosphorylation.
294

295 **Recombinant VHSV harboring M mutations**

296 Recombinant VHSV harboring the D62A and D62A/E181A mutations were generated using a
297 reverse genetic system (53). Recombinant viruses containing the mutant M genes were viable, and
298 were compared to recombinant wild type (rWT) VHSV in a series of cell-based studies. To assess
299 viral replication, EPC cells were infected for 0, 18, 36, 54, 72, or 96 h at a MOI = 0.1 or 1.0 with
300 either D62A, D62A/E181A, or rWT VHSV. Media and cells were harvested at each time point. A
301 viral yield assay was used to compare the ability of mutant viruses to replicate to that of rWT virus
302 by titering the media from each time point in 1:10 serial dilutions on Bluegill Fry (BF-2) cells. At
303 an MOI = 0.1, replication of rWT virus peaked at 54 h, while M D62A and M D62A/E181A
304 viruses peaked at 96 h and 72 h, respectively (Fig. 9A). M D62A virus replication was similar to
305 rWT virus at 72 h and then exceeded rWT titers at 96 h (Fig. 9A). M D62A/E181A virus yielded
306 titers that were several orders of magnitude less than that of rWT or M D62A viruses (Fig. 9A).
307 However, at MOI 1, all three viruses reach similar titers after 96 h (Fig. 9B), suggesting that other
308 factors affecting viral replication, such as viral cytotoxicity and restriction by the innate immune
309 response were impacted by these mutations.

310

311 **Transcriptional Inhibition by rWT VHSV and mutants**

312 The abilities of the rWT and mutant M containing viruses to suppress host transcription
313 were assessed first by using the constitutively active SV40/luc reporter. EPC cells were transfected
314 with the SV40/luc for 6 h and then infected for 24 h with each virus (MOI = 0.1 or 1), after which
315 luciferase activity was quantified. The rWT virus was 2- to 2.5-fold more effective at inhibiting
316 luciferase activity as compared to M D62A and M D62A/E181A viruses (Fig. 10A), mirroring the
317 impact of the transfected M proteins (see Fig. 8C). To examine the effect of mutant M and rWT
318 viruses on class II specific gene expression, EPC cells were infected with each of the three viruses
319 for 24 h at a MOI = 1. Cells were subjected to analysis by immunofluorescence microscopy using a
320 RNAP II phospho-serine-2 specific antibody as a surrogate for class II gene transcriptional activity,
321 with values quantified by a mean grey scale intensity within the nuclei (Fig. 10B, C). Anti-VHSV
322 staining, carried out in parallel cultures (due to secondary antibody conflict), indicated that virtually
323 all cells were infected. Only rWT virus significantly inhibited RNAP II phospho-serine-2 staining,
324 suggesting that the anti-transcriptional effects of M D62A and M D62A/E181A viruses were
325 markedly reduced as compared to rWT VHSV.

326

327 **Cytopathic effects of rWT VHSV and mutants**

328 The reduced transcriptional inhibitory activities of the M D62A and M D62A/E181A mutant
329 viruses suggested that induction of host cell cytopathicity was likely to be less severe for the mutant
330 viruses as compared to rWT VHSV. To assess the impact of viral titer on cytopathicity, EPC cells
331 were infected with each of the viruses for 96 h at MOIs ranging from 0.0001 to 10. After that time,
332 cells were fixed in trichloroacetic acid and stained with Sulforhodamine-B to quantify viable cells.
333 This assay showed that the mutant viruses induced significantly fewer cytopathic effects at MOI <
334 1.0 (Fig. 10D). Interestingly, in EPC cells infected with mutant M viruses, plaques formed that
335 initially appeared similar to those for rWT virus, but over the course of the experiment the mutant

336 virus plaques remained smaller than those generated by the rWT virus, and in some cases refilled
337 with cells after initial formation (Fig. 10E).

338 To monitor global cellular RNA synthesis, we again used the Click-iT chemistry reaction with
339 AlexaFluor-594 (AF-594) and 5-EU, and then assessed incorporation with both fluorescent
340 microscopy and flow cytometry. EPC cells were left untreated or were treated with Actinomycin-D
341 (1 h prior to EU addition) or infected with mutant or WT viruses (24 h). The 5-EU was added for
342 the last hour of treatment/infection, after which labeled cells were subjected to flow cytometry to
343 quantify EU positive versus negative cells (Fig. 11A-C, G-I). To ensure robust infection, cells on
344 coverslips from each treatment were subjected to immunofluorescence microscopy using a αVHSV
345 primary and a FITC conjugated goat-anti-rabbit secondary antibody after the Click-iT reaction was
346 completed (Fig. 11D-F, J-L). Flow cytometric data suggested that the mutant M containing viruses
347 were roughly 80% less effective at inhibiting host transcription as compared to rWT VHSV.

348

349 **Innate immune activation by VHSV rWT and mutants**

350 To determine how differences in transcriptional inhibition impacted antiviral activity release, media
351 collected from control or infected cells were UV irradiated to inactivate live virus and subjected to
352 IFN bioassay (Fig. 12). The mutant M viruses both elicited enhanced release of antiviral activity
353 (expressed in units IFN/mL; uIFN/mL) as compared to rWT VHSV. M D62A induced 1.9- and
354 22.5-fold more uIFN/mL than rWT at MOIs = 0.1 and 1, respectively, whereas the M D62A/E181A
355 virus induced 2.25- and 49.4-fold more uIFN/mL than rWT virus at MOIs = 0.1 and 1, respectively
356 (Fig. 12).

357 To determine whether the enhanced antiviral activity correlated with altered innate immune
358 gene expression, EPC cells were infected with M D62A, M D62A/E181A or rWT viruses for 96 h
359 at MOIs = 0.1 and 1, with both media and cells collected at 0, 4, 18, 36, 54, 72, and 96 h.p.i. cDNA
360 was made from RNA extracted from the collected cells that was spiked with 1.0 ng of *in vitro*
361 transcribed GFP RNA for normalization, since virus infection alone leads to suppression of host

362 RNA synthesis and would impact reference gene expression. Expression of IFN, IFN-responsive
363 Mx-1 and VHSV RNA was quantified with RT-qPCR (Fig. 13). At both MOIs, the M D62A virus
364 induced more IFN and Mx-1 transcription than the M D62A/E181A and rWT viruses. However,
365 when these values were normalized to the amount of viral RNA, the M D62A/E181A virus induced
366 5 and 4.5-fold more IFN and Mx-1 mRNA, respectively than the M D62A virus at MOIs = 1. The
367 mutant M viruses also consistently induced 10 fold more IFN mRNA than rWT virus at MOIs = 0.1
368 and 1, respectively. These data suggested that the mutant M viruses led to greater expression of IFN
369 throughout the course of infection when compared to rWT.
370

371 **Discussion**

372 Most viruses have evolved mechanisms to inhibit the expression or function of host innate
373 immune genes during virus replication (54,55). Inhibition of host transcription is a common
374 strategy used by RNA viruses that replicate entirely within cytoplasm. Shutting down host
375 transcription not only frees up cellular translational machinery that can be used for biosynthesis of
376 viral gene products, but it also inhibits the host antiviral responses by preventing synthesis of
377 antiviral proteins. One clear example of an anti-host protein found within the rhabdovirus family is
378 the VSV M protein, which potently inhibits host gene expression, thereby suppressing host antiviral
379 responses including upregulation of type I IFNs (56,57). VSV M also may block mRNA export
380 from the nucleus (47,48,58). These anti-host functions of VSV M are separable from its critical role
381 in viral assembly and budding, but are still essential for efficient viral replication (59-61). The
382 salmonid rhabdovirus IHNV M protein also inhibits host-directed gene expression (38).

383 Here we report that VHSV-IVb infection suppressed host IFN-mediated antiviral responses,
384 with expression of M alone capable of inhibiting MAVS-mediated IFN expression, as well as IFN-
385 mediated transcriptional responses in cell-based luciferase assays (Fig. 2). Importantly, viral
386 infection or transfected VHSV M also inhibited transcription from a constitutively active SV40
387 promoter driven luciferase construct (Fig. 3), suggesting that VHSV M acts similarly to other

388 rhabdoviral M proteins in shutting down general transcription and/or post-transcriptional events.
389 This possibility was enforced and clarified by the observation that VHSV infection or ectopic
390 expression of M led to decreased host nascent RNA transcription. Our results support the
391 hypothesis that VHSV M protein inhibits host transcription as a means of promoting viral
392 dissemination.

393 VSV M protein blocked host transcription directed by all three host RNA polymerases
394 (RNAP I-III: (44)). We tested the inhibitory potency of VHSV M on three different luciferase
395 constructs driven by the RNAP I-dependent Atlantic salmon ITS1 promoter, the RNAP II-
396 dependent SV40 promoter and the human RNAP III-dependent U6 promoter, respectively. VHSV
397 M co-transfection inhibited transcription mediated by all three RNA polymerases (Fig. 4).
398 Interestingly, EU staining of nascent RNA synthesis in VHSV-infected and M-transfected cells
399 resembled the pattern of α-Amanitin treatment (Fig. 4). Since α-Amanitin targets RNAP II and III,
400 but not RNAP I, this suggests that M may target all three host RNAPs through a common
401 mechanism, which may not be equally efficacious in all instances. Since continued rRNA synthesis
402 would benefit the virus, it is possible that residual RNAP I activity is an evolutionary outcome of
403 otherwise indiscriminate host RNAP suppression.

404 The mechanism of VHSV M transcriptional inhibition remains unclear. Previous studies of
405 VSV M suggested that the TATA-binding protein (TBP) subunit TFIID was a potential target of M.
406 TFIID isolated from VSV infected cells was inactive in an *in vitro* transcription assay, but
407 transcription activity could be reconstituted by adding purified recombinant TBP to the
408 experimental system (40). Our ChIP assay results implicated an M-dependent suppression of both
409 basal and doxycycline-induced recruitment of RNAP II to the minimal CMV promoter region of a
410 Tet-mSEAP reporter gene (Fig. 6). Taken together, our data suggest that VHSV M inhibited RNAP
411 II-directed transcription by interrupting RNAP II promoter binding, perhaps by targeting one or
412 more basal transcription factors. However, it remains uncertain whether this inhibition is direct, or
413 indirect via suppression of regulatory pathways involved in RNA polymerase synthesis and

414 subcellular transport. Future studies will need to address this question, however a possible role for
415 VHSV M in perturbation of nuclear import/export was revealed in our RNA localization studies
416 (Fig. 5). Although not conclusive, the increased nuclear to cytoplasmic ratios in VHSV infected
417 cells suggest additional similarities to VSV M function (47,48), and provides further evidence that
418 the observed effects of M on luciferase inhibition using our various constructs can be attributed to
419 pre-translational effects.

420 M proteins from a variety of VHSV strains and several closely related fish viruses,
421 including IHNV, SHRV and SVCV all inhibited SV40 promoter activity in EPC cells, which is
422 consistent with the suppression of host protein expression being a conserved role for M protein
423 among rhabdoviruses. Interestingly, a novel M clone isolated from a VHSV F1 strain (Ia substrain)
424 sample was less potent than other M proteins in inhibiting transcription (Fig. 7). When comparing
425 this F1 M sequence with that of WT IVb M, just four amino acids differences (T9I, D62G, E181A
426 and V198A) were present. We tested a range of targeted mutations at these positions and found that
427 G62D conversion in the Ia M clone enhanced function to approximately that of the IVb M (data not
428 shown). To further investigate the impact of the M alternatives (using more traditional alanine
429 substitutions), two mutant M constructs (D62A and D62A/E181A) were made within the IVb M
430 background. Both exhibited decreased ability to inhibit cellular gene expression as compared to
431 WT IVb M (Fig. 8). The predicted secondary structure of VHSV M is quite similar to that of VSV
432 M even though amino acid conservation between the two is low (data not shown). The aspartic acid
433 residue at position 62 is conserved across multiple VSV and VHSV strains (62). In the VSV M
434 protein, this aspartic acid (D92) is located between helices α1 and α2, and is surface exposed (62).
435 It may play a critical role in the anti-host function of M by serving in a structural capacity, or as a
436 site for protein-protein interactions with host factors involved in regulating transcription.
437 Regardless, conservation of this aspartic acid residue across viruses is striking, and worthy of
438 additional investigations.

439 The two M protein point mutants (M D62A and M D62A/E181A) that exhibited

440 significantly reduced anti-transcriptional potential in cell-based studies (Fig. 8) were incorporated
441 into an rWT VHSV backbone, using a reverse genetic system. The primary goal was to determine if
442 the M mutants would support M's critical functions in viral replication, and if so, whether anti-host
443 functions of the resulting viruses were impacted. Both M D62A and M D62A/E181A viruses were
444 viable, which allowed us to investigate the abilities of these mutant viruses to replicate, elicit
445 cytotoxic effects, inhibit host transcription and/or otherwise modulate host gene expression. The M
446 D62A/E181A virus exhibited reduced replicative capabilities at an MOI 0.1 as compared to the WT
447 and D62A viruses (Fig. 9). These data suggested that the D62A/E181A mutation, but not the D62A
448 mutation alone, elicited a restrictive effect on propagation, perhaps implicating a role for E181 in
449 viral packaging or budding. For VSV M, F208 is structurally homologous to VHSV M E181 and
450 helps coordinate the positioning of a superiorly located α-helix that forms the border of the
451 hydrophobic pocket VSV M utilizes in multimerization during viral skeleton formation (63). Thus,
452 loss of electron density at this position could allow for a larger degree of freedom in the superior α-
453 helix, leading to a malformed hydrophobic pocked and deficient polymerization, and thus reduced
454 replication. However, the most striking effects of the D62A and D62A/E181A mutations were their
455 reduced abilities to suppress transcriptional responses in EPC cells (Figs. 8, 10, 11 and 13). As
456 such, an alternative explanation for the reduced replication of the double mutant might be that
457 enhanced IFN production in infected cells was capable of restricting propagation so effectively that
458 the virus could not spread far beyond the initially infected cells, particularly if replication was even
459 slightly delayed.

460 Although the D62A virus fared better than the double mutant in viral yield assays, its
461 inability to suppress gene expression led to decreased cytopathicity and plaque spread at low MOI
462 (Fig. 10). Since the D62 residue is highly conserved among rhabdoviruses, we would predict that it
463 is structurally or functionally important. Molecular modeling predicted that residue D62 of VHSV
464 M is in a random coil located proximal to the globular domain (64). Mutations within this region
465 impacted the localization of VSV M (65), suggesting that the D62A mutation may have affected the

466 ability of M D62A mutants to localize properly, as opposed to causing a more general loss in
467 structural integrity. Other functions have been ascribed to the orthologous region of the VSV M
468 protein, including regulation of membrane association (66) and protein turnover (59), although both
469 of those studies utilized larger deletions or multiple amino acid mutations as compared to the point
470 mutation here. Outside of this specific coil domain, the N-terminus of VSV M has been implicated
471 in other aspects of host inhibition, including association with RAE1/NUP98 (45,48) or suppression
472 of eIF2α phosphorylation (M51R) (67). Whether VHSV M also engages these conserved proteins
473 and/or whether D62A mutations impact these same cellular functions, directly or indirectly, will
474 have to await future studies.

475 Overall, our data provide insight into the various and critical roles of VHSV M protein in
476 viral replication and host suppression. The findings are consistent with many previous studies of
477 VSV M, and confirm a conserved role for M in host suppression among many rhabdoviruses. Our
478 results show that, like VSV M, the anti-host functions of VHSV M can be uncoupled from the viral
479 packaging functions, and as such lays the groundwork for studies directed towards developing
480 disabled or attenuated recombinant viruses useful in host response and/or immunization studies, as
481 well as more in-depth functional analyses of the mechanisms behind the observed biological effects
482 of VHSV M and its mutants.

483

484 **Materials and Methods**

485 **Cell lines and culture conditions**

486 *Epithelioma papulosum cyprinid* (EPC) cells were purchased from the American Type
487 Culture Collection (ATCC, Rockville, MD; CRL-2872). The cells were grown in Eagle's Minimum
488 Essential Medium (EMEM) (Fisher) supplemented with 10% fetal bovine serum (FBS) (Invitrogen,
489 Carlsbad, CA) and 1% penicillin/streptomycin (Invitrogen) (complete EMEM) at 22° C in a 5%
490 CO_2 enriched environment. Human Embryonic Kidney (HEK)-293 cells were purchased from
491 ATCC (CRL-1573), grown in complete Dulbecco's MEM at 37° C in a 5% CO_2 enriched

492 environment. α-Amanitin (Santa Cruz Biotechnology, Inc. CA) and Actinomycin-D (Sigma-
493 Aldrich, St. Louis, MO) were used at a final concentration of 1 μg/ml, while Leptomycin B (LMB)
494 was used at 10 μg/ml.
495
496 **Plasmids**
497 Expression vectors for EPC MAVS and EPC IFN were obtained from Dr. Michel Brémont
498 (French National Institute for Agricultural Research, Jouy-en-Josas Cedex, France), the VHSV L
499 expression plasmid was reported previously (53), the Tet-mSEAP construct was obtained from Dr.
500 Fan Dong (University of Toledo, Toledo, USA) and the IFN-luciferase reporter was obtained from
501 Dr. John Hiscott (Istituto Pasteur-Fondazione Cenci Bolognetti, Rome, Italy). Other plasmids used
502 included the IFN-induced transmembrane-1 (IFITM-1)/luc plasmid, derived from the pDW9-
503 27CD2, SV40/βgal (Promega), SV40/luc (modified from SV40/βgal). VHSV-IVb M, NV, G, and
504 N coding sequences were PCR amplified with appropriate primers (Table 1). All fragments were
505 cloned into pcDNA 3.1 (-) myc/his A (Invitrogen), or p3xFLAG-CMV-14 (Sigma-Aldrich). IHNV,
506 SVCV and SHRV M cDNAs were PCR cloned from viral stocks using targeted primers (Table 1).
507 Luciferase driven by human U6 promoter reporter construct (pGL3-U6-Luc) was generated
508 by subcloning human U6 promoter from pLKO.1 puro vector (Addgene plasmid # 10879) into
509 pGL3 luciferase reporter vector (Promega #E1751) upstream of luciferase gene using Gibson
510 Assembly (NEB #E5520). Rainbow trout RNAP I promoter luciferase construct (pGL3-ITS1-Luc)
511 was generated by subcloning rainbow trout rRNA intergenic sequence region ITS1 into pGL3
512 luciferase reporter vector between two Hind III sites.
513
514 **Recombinant virus production.**
515 Construction of a full-length infectious clone of VHSV has been described earlier (68). This clone
516 was used as a backbone to introduce desired mutations in the M gene, which is flanked by unique
517 *Nhe*I and *Pvu*II restriction sites in the full-length clone. To construct plasmid pVHSV-D62A,

518 primers were designed to effect Asp to Ala mutation at amino acid position 62 (D62A) in the M
519 protein, and used in PCR along with flanking *Nhe*I-forward and *Pvu*II-reverse primer to amplify a
520 PCR fragment of 712 bp. The obtained PCR product was subjected to DNA sequencing to confirm
521 the presence of introduced mutation (D62A). This fragment was double digested with *Nhe*I and
522 *Pvu*II restriction enzymes and cloned between *Nhe*I-*Pvu*II sites of the full-length VHSV clone. To
523 construct plasmid pVHSV-D62A/E181A, another set of primers were used to effect the Glu to Ala
524 mutation at position 181 of the M protein. Using the single mutant cDNA fragment as a template,
525 another PCR was carried out with the flanking *Nhe*I-forward and *Pvu*II-reverse primers to obtain a
526 PCR product of 712-bp. DNA of the PCR product was sequenced to confirm the presence of two
527 mutations (D62A/E181A). This product was double digested with *Nhe*I-*Pvu*II and cloned into the
528 full-length VHSV clone, as described above.

529 To generate recombinant viruses, EPC cells were transfected with plasmids pVHSV-D62A and
530 pVHSV-D62A/E181A along with the support plasmids, using a protocol described earlier (69).
531 Briefly, plasmids pVHSV or its derivatives were diluted in 500 µl Opti-MEM medium. Next,
532 Lipofectamine LTX reagent (Invitrogen) was added, according to manufacturer's instructions, and
533 incubated for 30 min at room temperature. The plasmid–Lipofectamine reaction mixture was added
534 to the EPC monolayer in a six-well plate without replacing the growth medium. The transfection
535 mixture was removed after 8 h of incubation at 28° C, and the transfected cells were washed and
536 maintained in Eagle's MEM containing 10% FBS at 14° C for 5 d. Cell monolayer was observed
537 for the development of virus-induced CPE. After 5 d of incubation, the cells were submitted to
538 three cycles of freeze thawing. Supernatant was clarified at 8,000 × *g* in a microcentrifuge and used
539 to inoculate fresh cell monolayers in T-25 flasks at 14° C. The supernatant was harvested and
540 clarified for further characterization of the recombinant viruses. To verify that recovered viruses
541 contain the introduced mutations, genomic RNA was extracted from partially purified virus using
542 an RNeasy Mini Kit (Qiagen, Hilden, Germany), and subjected to reverse transcription to obtain
543 cDNA fragments of the VHSV genome, which were sequenced completely to confirm the presence

544 of introduced mutations in the M gene.

545

546 **VHSV Amplification and Purification**

547 The VHSV-IVb MI03GL isolate was kindly provided by Dr. James Winton (United States
548 Geological Survey, Seattle, Washington). VHSV F1strain was kindly provided by Dr. Gale Kurath
549 (United States Geological Survey, Seattle, Washington). VHSV-IVb isolates and recombinant
550 viruses were amplified for subsequent purification by infecting a confluent monolayer of BF-2 cells
551 in a 15 cm tissue culture dish with a 1:1000 (v/v) dilution of un-purified virus stock in serum-free
552 EMEM. Viral adsorption was allowed to proceed for 1 h before virus-containing media was
553 replaced with complete EMEM. Virus was cultured until the onset of cytopathicity was observed
554 (72 h). Virus containing media and attached cells were subjected to a freeze-thaw cycle before the
555 removal of cell debris by low speed centrifugation (4,000 × *g*, 30 min). The resulting supernatant
556 was clarified using a 0.22 µm syringe-tip filter, then subjected to ultra-centrifugation through a
557 25% (w/v) sucrose pad at 25,000 rpm for 3 h at 4° C. The virus-containing pellet was resuspended
558 overnight at 4° C in PBS. Virus stocks were titered by 1:10 serial dilutions using confluent EPC
559 cells then divided into 100 µL aliquots and stored at -80° C until use.

560

561 **Virus Yield and IFN-Bioassays**

562 To assess viral replication, EPC cells were infected for 0, 4, 18, 36, 54, 72, or 96 h at a MOI = 0.1
563 or 1.0 with either M D62A, M D62A/E181A, or rWT VHSV. Media and cells were harvested at
564 each time point. A viral yield assay was used to compare the ability of mutant viruses to replicate to
565 that of rWT virus by titering the media from each time point in 1:10 serial dilutions on BF-2 cells.
566 At 72 h.p.i., plaques were counted and a final viral concentration in plaque forming units per mL
567 (pfu/mL) was calculated for each time point. Antiviral assays were completed using UV irradiated
568 media (70 mJ/cm^2) from each time point which was applied overnight to EPC cells in 1:3 serial
569 dilutions. Cells treated with irradiated media were subjected to virus challenge using sucrose

570 purified rWT VHSV for 72 h and then were fixed and stained with crystal violet. Stained wells
571 were dried overnight and dye was dissolved with 30% (v/v) acetic acid for spectrophotometric
572 quantification. Absorbance values of treated wells were normalized to values obtained by untreated
573 and uninfected wells and 1 unit of IFN was defined as the amount necessary to provide 50%
574 protection from virus CPE.
575
576 **Transfection**
577 EPC cell transfections were performed by using Polyjet reagent (SignaGen, Gaithersburg,
578 MD) following the manufacturer's instructions. Briefly, plasmids were mixed with Polyjet in
579 serum-free EMEM for 20 min then added to cells in serum-free medium. Media were changed to
580 complete medium after 3 h incubation. Plasmid concentrations in all transfection experiments were
581 equalized between samples by inclusion of empty vector.
582
583 **Click-iT RNA Alexa Fluor 594 Imaging and Immunofluorescence Microscopy**
584 Click-iT reactions were performed using a Click-iT RNA Imaging Kit (Invitrogen). For
585 fluorescent microscopy, cells were seeded on Poly-L-Lysine coated coverslips in a 6-well culture
586 dish and grown to ~70% confluence. For flow cytometry, cells were plated identically, but without
587 coverslips. Wells were then infected with either rWT, M D62Aor M D62A/E181A viruses at a
588 MOI = 1.0 for 24 h. At 23 h.p.i., an uninfected well was treated with Actinomycin-D (1 µg/mL) for
589 1 h before 5-ethynyl uridine (EU) was added to all wells to a final concentration of 1 mM. Cells
590 were allowed to incorporate EU for 1 h before monolayers were washed with PBS and coverslips
591 removed. Cells remaining on the plate were harvested by the addition of Versene (0.02% (w/v)
592 EDTA in PBS) and centrifuged at 700 × *g* for 5 min at 4° C. Cells on coverslips and in Eppendorf
593 tubes were fixed and permeabilized by the addition of Fixation Buffer [4.0% (w/v)
594 Paraformaldehyde in TBST (pH = 7.5)] for 30 min at room temperature. Cells were washed once
595 with 100 mM Glycine in PBS to quench paraformaldehyde induced auto-fluorescence, and then

596 once in PBS. Cells were incubated with in Click-iT reaction cocktail for 30 min at room
597 temperature in the dark then washed with Click-iT reaction rinse buffer. For immunofluorescent co-
598 staining, cells on coverslips were blocked for 30 min at room temperature (1% BSA in PBS), then
599 with primary antibody (in 1% BSA in PBS) for 1 h. Cells were washed in PBS 3 times for 5 min
600 each, then FITC conjugated secondary antibody conjugated (in 1% BSA in PBS) was added for 1 h
601 at room temperature. After a PBS wash, the cover slips were mounted to slides with ProLong Gold
602 Antifade Mountant with DAPI (Life Technologies, Carlsbad, CA) for 24 h, then imaged on an
603 Olympus IX81 inverted fluorescent microscope. For flow cytometric analysis, cells were pelleted,
604 then resuspended in 1% (w/v) BSA and incubated at 4° C in the dark until flow cytometry data
605 collection using a BD Scientific LSRFortessa using the Allophycocyanin (APC) 650/660 nm
606 excitation/emission filter. Flow data were then analyzed using the FLOWJO Single Cell Analysis
607 Software v.10. (BD Biosciences, San Jose, CA)
608
609 **Luciferase assays/β-gal assays**
610 Cells were transfected with the appropriate plasmids in 12-well tissue culture plate at a
611 density ~70% for 24 or 48 h. After media removal, cells were washed with PBS twice then lysed
612 for 15 min on ice in 150 µl Cell Culture Lysis Reagent 5× (diluted to 1× in water) (Promega,
613 Madison, WI). Half of the clarified lysate was used to assess luciferase activity while the other half
614 was used for β-galactosidase activity determination using 50 µl β-gal buffer (60 mM Na_2HPO_4, 40
615 mM NaH_2PO_4, 10 mM KCl, 2 mM $MgSO_4$, 2.6 µM ortho-Nitrophenyl-β-D-galactopyranoside, 3.2
616 µl β-mercaptoethanol). The mixture was incubated 1 h at 37°C and then absorbance read at 414 nm
617 using a plate reader (SpectraMax, Molecular Devices, Sunnyvale, CA). The luciferase reading was
618 normalized to the β-gal reading. To obtain a fold induction value, each values of sample was
619 normalized to the value of negative control.
620
621 **Cell fractionation**

622 Cells transiently transfected with pCD-M were fractionated into nuclear membrane (NM), soluble
623 nuclear (SN), mitochondrial (M) and cytoplasmic (C) fractions using differential centrifugation.
624 Briefly, three 10 cm plates were transfected with pCD-M. The following day, cells were scraped
625 from the plate and resuspended in 5 vol mitochondrial isolation buffer (220 mM mannitol, 68 mM
626 sucrose, 10 mM HEPES pH 7.4, 10 mM KCl, 1 mM EGTA, 1 mM EDTA, 1 mM MgCl2). Cells
627 were incubated for 5 min on ice and then dounce homogenized. Homogenate was centrifuged for
628 10 min at 1000g. The supernatant was further centrifuged for 10 min. at 10,000g providing the
629 mitochondrial pellet and cytoplasmic fraction (supernatant). The previous pellet was resuspended
630 with RIPA lysis buffer (150 mM NaCl, 1% NP-40, 0.5% sodium deoxycholate, 0.1% SDS, 50 mM
631 Tris pH 8.0, 1 mM PMS) and incubated on ice for 15 min. Finally the lysate was centrifuged at
632 10,000g for 10 min. to provide the nucleoplasm and nuclear membrane extracts. Both final pellet
633 fractions were washed three times with the buffer used in the previous step.
634

635 **Immunoblotting**

636 Cell lysate was separated by sodium dodecyl sulfate polyacrylamide gel electrophoresis
637 (SDS-PAGE) as previously described (69). Briefly, samples were run on 12.5% gel. Proteins then
638 were transferred to Immobilon-P Polyvinylidene Fluoride (PVDF) membrane and blocked in 1%
639 BSA in TBST. Membranes were incubated overnight with primary antibody (1:1000 in 1% BSA in
640 TBST) at 4°C, membranes washed in TBST then incubated with secondary antibody conjugated
641 with HRP in 1% BSA in TBST (1 h at room temperature). Membranes were washed in TBST and
642 incubated with Enhanced Chemiluminescence reagent (Pierce, Rockford, IL) for 2 min then
643 visualized using UVP ChemiDoc-It^2 510 Imager.
644

645 **Real-time qPCR**

646 EPC cells transfected with various plasmids or infected with indicated viruses were subjected to
647 RNA isolation using TRIzol (Invitrogen), according to the manufacturer's protocol. Moloney

648 Murine Leukemia Virus Reverse Transcriptase (M-MLV-RT) (Promega, Madison, WI) was used to
649 reverse transcribe 1 μg of isolated RNA. Reverse transcription reactions were carried out by
650 incubating 1 μg of RNA with 100 ng of random hexamer primer and water to a total volume of 7
651 μL at 70° C for 10 min. For RT-qPCR studies with recombinant viruses, 1 ng of *in vitro* transcribed
652 GFP RNA also was added to the reaction to serve as an internal control for normalization, since
653 virus infection itself shuts down endogenous RNA synthesis. Reactions were briefly cooled to 4° C
654 before adding 13 μL of M-MLV-RT mixture [4 μL M-MLV-RT 5x reaction buffer, 2 μL of 5 mM
655 dNTPs (Invitrogen), 0.5 μL M-MLV-RT (Promega), and water to 13 μL]. Samples then were
656 incubated 1 h at 42° C, cDNA samples diluted 1:10 with water then subjected to qPCR using GFP,
657 EPC β-actin, VHSV M, Mx-1, and EPC IFN primers (Table 1). RT-qPCR was performed using 5
658 μL of Radiant Green Lo-ROX 2× qPCR kit (Alkali Scientific, Pompona Beach, FL), 1 μL diluted
659 cDNA, 50 ng of each primer, and water to a total volume of 10 μL. Reactions and data collection
660 were performed with a Bio-Rad C1000 Real Time Thermocycler for 3 min initial denaturation at
661 95° C, followed by 40 cycles of 15 s 95° C denaturation and 30 s 60° C elongation. Readings were
662 taken at the end of each elongation step. Threshold numbers were obtained by an automated single
663 point threshold within the log-linear range. Samples were normalized to EPC β-actin or GFP, and
664 relative gene expression levels were calculated using the $2^{-\Delta\Delta CT}$ method.

665

666 **ChIP Assay**

667 The chromatin immunoprecipitation (ChIP) assay was performed as previously described
668 with the following modifications (70). Briefly, 10^7 cells were cross-linked with 1% formaldehyde
669 for 10 minutes and then quenched with 125 mM glycine for 5 minutes at room temperature. Nuclei
670 were prepared in Cell Lysis Buffer (5 mM Tris-HCl pH 8, 85 mM KCl, 0.5% NP-40, 0.5 mM
671 PMSF, 1X protease inhibitor cocktail (PIC, Thermo Scientific) on ice for 10 minutes and sonicated
672 to yield chromatin fragments (200 to 700 bp). Immunoprecipitations were performed overnight at 4
673 °C using 1 μg of anti-RNAP II a A304-405A (Bethyl Laboratories, Montgomery, TX) or IgG, and

674 then incubated with protein A agarose (EMD Millipore, Billerica, MA), which was pre-equilibrated
675 with sonicated herring sperm DNA and BSA. Immunoprecipitated material was washed
676 extensively, and the cross-links were reversed. DNA from the eluted chromatin was purified by
677 PCR purification kit following manufacturer's instructions (Qiagen). Differences in DNA
678 enrichment for ChIP samples were determined by qPCR using 4% of the precipitated sample DNA
679 and 1% of the input DNA. The primers used for ChIP assay are listed in Table 1.
680

681 **Statistics**

682 Data management, analysis, and graphing was done in Microsoft Excel 2016. Analysis was
683 performed by two-tailed, unpaired Student's t-tests. Graphs represent the statistical mean ±
684 standard error of the mean (SEM).
685

686 **Acknowledgements:** This manuscript benefitted from critical comments provided by anonymous
687 reviewers. This study was funded by NSF DBI-1354806/1354684 (D.W.L, C.A.S., V.N.V.) and
688 USDA/ARS CRIS project # 5090-31320-004-00D, under specific cooperative agreement #58-
689 3655-9-748 (D.W.L., C.A.S.). The views contained in this document are those of the authors and
690 should not be interpreted as necessarily representing the official policies, either expressed or
691 implied, of the U.S. Government. Mention of trade name, proprietary product, or specific
692 equipment does not constitute a guarantee or warranty by the USDA and does not imply its
693 approval to the exclusion of other products that may be suitable. This manuscript is submitted for
694 publication with the understanding that the United States Government is authorized to reproduce
695 and distribute reprints for governmental purposes. The authors would also like to thank Shelby
696 Powell, Tyler Williams, Tyler Popil and Jacob Blandford for technical assistance with some of the
697 experiments described herein. PMEL contribution number 4623.
698

699 **REFERENCES**

700 1. Janeway, C.A., 1989. Approaching the asymptote? Evolution and revolution in immunology.
701 Cold Spring Harbor symposia on quantitative biology 54, 1-13.
702 2. Janeway Jr, C.A., Medzhitov, R., 2002. Innate immune recognition. Annual review of
703 immunology 20, 197-216.
704 3. Loo, Y.M., Gale, M., Jr., 2011. Immune signaling by RIG-I-like receptors. Immunity 34, 680-
705 692.
706 4. Kawai, T., Takahashi, K., Sato, S., Coban, C., Kumar, H., Kato, H., Ishii, K.J., Takeuchi, O.,
707 Akira, S., 2005. IPS-1, an adaptor triggering RIG-I- and Mda5-mediated type I interferon
708 induction. Nat Immunol 6, 981-988.
709 5. Lin, R., Mamane, Y., Hiscott, J., 1999. Structural and functional analysis of interferon regulatory
710 factor 3: localization of the transactivation and autoinhibitory domains. Mol Cell Biol 19,
711 2465-2474.
712 6. Seth, R.B., Sun, L., Ea, C.K., Chen, Z.J., 2005. Identification and characterization of MAVS, a
713 mitochondrial antiviral signaling protein that activates NF-kappaB and IRF 3. Cell 122,
714 669-682.
715 7. Yoneyama, M., Suhara, W., Fukuhara, Y., Fukuda, M., Nishida, E., Fujita, T., 1998. Direct
716 triggering of the type I interferon system by virus infection: activation of a transcription
717 factor complex containing IRF-3 and CBP/p300. EMBO J 17, 1087-1095.
718 8. Platanias, L.C., 2005. Mechanisms of type-I- and type-II-interferon-mediated signalling. Nat Rev
719 Immunol 5, 375-386.
720 9. Stark, G.R., 2007. How cells respond to interferons revisited: from early history to current
721 complexity. Cytokine Growth Factor Rev 18, 419-423.
722 10. Galabov, A.S., 1981. Induction and characterization of tortoise interferon. Methods Enzymol
723 78, 196-208.
724 11. Altmann, S.M., Mellon, M.T., Distel, D.L., Kim, C.H., 2003. Molecular and functional analysis
725 of an interferon gene from the zebrafish, Danio rerio. J Virol 77, 1992-2002.

726 12. Schultz, U., Kaspers, B., Staeheli, P., 2004. The interferon system of non-mammalian
727 vertebrates. Dev Comp Immunol 28, 499-508.

728 13. Zou, J., Tafalla, C., Truckle, J., Secombes, C.J., 2007. Identification of a second group of type I
729 IFNs in fish sheds light on IFN evolution in vertebrates. J Immunol 179, 3859-3871.

730 14. Sun, B., Robertsen, B., Wang, Z., Liu, B., 2009. Identification of an Atlantic salmon IFN
731 multigene cluster encoding three IFN subtypes with very different expression properties.
732 Dev Comp Immunol 33, 547-558.

733 15. Zou, J., Gorgoglione, B., Taylor, N. G. H., Summathed, T., Lee, P-T., Panigrahi, A., Genet, C.,
734 Chen, Y.-M., Chen, T.-Y., Ul Hassan, M., Mughal, S. M., Boudinot, P., Secombes, C. J.,
735 2014. Salmonids have an extraordinary complex Type I IFN system: characterization of the
736 IFN locus in rainbow trout Oncorhynchus mykiss reveals two novel IFN subgroups. J
737 Immunol 193 (5), 2273-2286.

738 16. Chang, M., Collet, B., Nie, P., Lester, K., Campbell, S., Secombes, C.J., Zou, J., 2011.
739 Expression and functional characterization of the RIG-I-like receptors MDA5 and LGP2 in
740 Rainbow trout (Oncorhynchus mykiss). J Virol 85, 8403-8412.

741 17. Biacchesi, S., LeBerre, M., Lamoureux, A., Louise, Y., Lauret, E., Boudinot, P., Bremont, M.,
742 2009. Mitochondrial antiviral signaling protein plays a major role in induction of the fish
743 innate immune response against RNA and DNA viruses. J Virol 83, 7815-7827.

744 18. Verrier, E.R., Langevin, C., Benmansour, A., Boudinot, P., 2011. Early antiviral response and
745 virus-induced genes in fish. Dev Comp Immunol 35, 1204-1214.

746 19. Manual of Diagnostic Tests for Aquatic Animals. In *Manual of Diagnostic Tests for Aquatic*
747 *Animals.* The World Organisation for Animal Health; 2016

748 20. Einer-Jensen, K., Ahrens, P., Forsberg, R., Lorenzen, N., 2004. Evolution of the fish
749 rhabdovirus viral haemorrhagic septicaemia virus. J Gen Virol 85, 1167-1179.

750 21. Schutze, H., Mundt, E., Mettenleiter, T.C., 1999. Complete genomic sequence of viral
751 hemorrhagic septicemia virus, a fish rhabdovirus. Virus Genes 19, 59-65.

752 22. Ammayappan, A., Vakharia, V.N., 2009. Molecular characterization of the Great Lakes viral
753 hemorrhagic septicemia virus (VHSV) isolate from USA. Virol J 6, 171.
754 23. Snow, M., Cunningham, C.O., Melvin, W.T., Kurath, G., 1999. Analysis of the nucleoprotein
755 gene identifies distinct lineages of Viral Haemorrhagic Septicaemia virus within the
756 European marine environment. Virus Res 63(1/2): 35-44.
757 24. Pierce, L.R., Stepien, C.A., 2012. Evolution and biogeography of an emerging quasispecies:
758 diversity patterns of the fish Viral Hemorrhagic Septicemia virus (VHSv). Mol Phylogenet
759 Evol 63, 327-341.
760 25. Stone, D.M., Ferguson, H.W., Tyson, P.A., Savage, J., Wood, G., Dodge, M.J., Woolford, G.,
761 Dixon, P.F., Feist, S.W., Way, K., 2008. The first report of viral haemorrhagic septicaemia
762 in farmed rainbow trout, Oncorhynchus mykiss (Walbaum), in the United Kingdom. J Fish
763 Dis 31, 775-784.
764 26. Toplak, I., Hostnik, P., Rihtaric, D., Olesen, N.J., Skall, H.F., Jencic, V., 2010. First isolation
765 and genotyping of viruses from recent outbreaks of viral haemorrhagic septicaemia (VHS)
766 in Slovenia. Dis Aquat Organ 92, 21-29.
767 27. Elsayed, E., Faisal, M., Thomas, M., Whelan, G., Batts, W., Winton, J., 2006. Isolation of viral
768 haemorrhagic septicaemia virus from muskellunge, Esox masquinongy (Mitchill), in Lake
769 St Clair, Michigan, USA reveals a new sublineage of the North American genotype. J Fish
770 Dis 29, 611-619.
771 28. Lumsden, J.S., Morrison, B., Yason, C., Russell, S., Young, K., Yazdanpanah, A., Huber, P.,
772 Al-Hussinee, L., Stone, D., Way, K., 2007. Mortality event in freshwater drum Aplodinotus
773 grunniens from Lake Ontario, Canada, associated with viral haemorrhagic septicemia virus,
774 type IV. Dis Aquat Organ 76, 99-111.
775 29. Groocock, G.H., Getchell, R.G., Wooster, G.A., Britt, K.L., Batts, W.N., Winton, J.R., Casey,
776 R.N., Casey, J.W., Bowser, P.R., 2007. Detection of viral hemorrhagic septicemia in round
777 gobies in New York State (USA) waters of Lake Ontario and the St. Lawrence River. Dis

Aquat Organ 76, 187-192.

30. Gagne, N., Mackinnon, A.M., Boston, L., Souter, B., Cook-Versloot, M., Griffiths, S., Olivier, G., 2007. Isolation of viral haemorrhagic septicaemia virus from mummichog, stickleback, striped bass and brown trout in eastern Canada. J Fish Dis 30, 213-223.

31. Thompson, T.M., Batts, W.N., Faisal, M., Bowser, P., Casey, J.W., Phillips, K., Garver, K.A., Winton, J., Kurath, G., 2011. Emergence of Viral hemorrhagic septicemia virus in the North American Great Lakes region is associated with low viral genetic diversity. Dis Aquat Organ 96, 29-43.

32. Cornwell, E.R., Eckerlin, G.E., Getchell, R.G., Groocock, G.H., Thompson, T.M., Batts, W.N., Casey, R.N., Kurath, G., Winton, J.R., Bowser, P.R., 2011. Detection of viral hemorrhagic septicemia virus by quantitative reverse transcription polymerase chain reaction from two fish species at two sites in Lake Superior. J aquat animal health 23, 207-217.

33. Kim, R., Faisal, M., 2010. Comparative susceptibility of representative Great Lakes fish species to the North American viral hemorrhagic septicemia virus Sublineage IVb. Dis Aquat Organ 91, 23-34.

34. Kim, R., Faisal, M., 2011. Emergence and resurgence of the viral hemorrhagic septicemia virus (Novirhabdovirus, Rhabdoviridae, Mononegavirales). Journal of Advanced Research 2, 9-23.

35. Ammayappan, A., Vakharia, V.N., 2011. Nonvirion protein of novirhabdovirus suppresses apoptosis at the early stage of virus infection. J Virol 85, 8393-8402.

36. Choi, M.K., Moon, C.H., Ko, M.S., Lee, U.-H., Cho, W.J., Cha, S.J., Do, J.W., Heo, G.J., Jeong, S.G., Hahm, Y.S., 2011. A nuclear localization of the infectious haematopoietic necrosis virus NV protein is necessary for optimal viral growth. PLoS One 6, e22362.

37. Kim, M.S., Kim, K.H., 2013. The role of viral hemorrhagic septicemia virus (VHSV) NV gene in TNF-alpha- and VHSV infection-mediated NF-kappaB activation. Fish Shellfish Immunol 34, 1315-1319.

804 38. Chiou, P.P., Kim, C.H., Ormonde, P., Leong, J.A., 2000. Infectious hematopoietic necrosis
805 virus matrix protein inhibits host-directed gene expression and induces morphological
806 changes of apoptosis in cell cultures. J Virol 74, 7619-7627.
807 39. Stepien, C.A., Pierce, L.R., Leaman, D.W., Niner, M.D., Shepherd, B.S., 2015. Gene
808 Diversification of an Emerging Pathogen: A Decade of Mutation in a Novel Fish Viral
809 Hemorrhagic Septicemia (VHS) Substrain since Its First Appearance in the Laurentian
810 Great Lakes. PLoS One 10, e0135146.
811 40. Yuan, H., Yoza, B.K., Lyles, D.S., 1998. Inhibition of host RNA polymerase II-dependent
812 transcription by vesicular stomatitis virus results from inactivation of TFIID. Virology 251,
813 383-392.
814 41. Tornoe, C.W., Christensen, C., Meldal, M., 2002. Peptidotriazoles on solid phase: [1,2,3]-
815 triazoles by regiospecific copper(i)-catalyzed 1,3-dipolar cycloadditions of terminal alkynes
816 to azides. J Org Chem 67, 3057-3064.
817 42. Rostovtsev, V.V., Green, L.G., Fokin, V.V., Sharpless, K.B., 2002. A stepwise huisgen
818 cycloaddition process: copper(I)-catalyzed regioselective "ligation" of azides and terminal
819 alkynes. Angew Chem Int Ed Engl 41, 2596-2599.
820 43. Dixon, P., Feist, S., Kehoe, E., Parry, L., Stone, D., Way, K., 1997. Isolation of viral
821 haemorrhagic septicaemia virus from Atlantic herring Clupea harengus from the English
822 Channel. Dis Aquat Organ 30, 81-89.
823 44. Ahmed, M., Lyles, D.S., 1998. Effect of vesicular stomatitis virus matrix protein on
824 transcription directed by host RNA polymerases I, II, and III. J Virol 72, 8413-8419.
825 45. Faria, P.A., Chakraborty, P., Levay, A., Barber, G.N., Ezelle, H.J., Enninga, J., Arana, C., van
826 Deursen, J., Fontoura, B.M., 2005. VSV disrupts the Rae1/mrnp41 mRNA nuclear export
827 pathway. Mol Cell 17, 93-102.
828 46. Her, L.S., Lund, E., Dahlberg, J.E., 1997. Inhibition of Ran guanosine triphosphatase-
829 dependent nuclear transport by the matrix protein of vesicular stomatitis virus. Science 276,

830 1845-1848.

831 47. Petersen, J.M., Her, L.S., Varvel, V., Lund, E., Dahlberg, J.E., 2000. The matrix protein of
832 vesicular stomatitis virus inhibits nucleocytoplasmic transport when it is in the nucleus and
833 associated with nuclear pore complexes. Mol Cell Biol 20, 8590-8601.

834 48. von Kobbe, C., van Deursen, J.M., Rodrigues, J.P., Sitterlin, D., Bachi, A., Wu, X., Wilm, M.,
835 Carmo-Fonseca, M., Izaurralde, E., 2000. Vesicular stomatitis virus matrix protein inhibits
836 host cell gene expression by targeting the nucleoporin Nup98. Mol Cell 6, 1243-1252.

837 49. Corden, J.L., 1990. Tails of RNA polymerase II. Trends Biochem Sci 15, 383-387.

838 50. O'Brien, T., Hardin, S., Greenleaf, A., Lis, J.T., 1994. Phosphorylation of RNA polymerase II
839 C-terminal domain and transcriptional elongation. Nature 370, 75-77.

840 51. Bensaude, O., Bonnet, F., Casse, C., Dubois, M.F., Nguyen, V.T., Palancade, B., 1999.
841 Regulated phosphorylation of the RNA polymerase II C-terminal domain (CTD). Biochem
842 Cell Biol 77, 249-255.

843 52. Komarnitsky, P., Cho, E.J., Buratowski, S., 2000. Different phosphorylated forms of RNA
844 polymerase II and associated mRNA processing factors during transcription. Genes Dev 14,
845 2452-2460.

846 53. Ammayappan, A., Kurath, G., Thompson, T.M., Vakharia, V.N., 2011. A reverse genetics
847 system for the Great Lakes strain of viral hemorrhagic septicemia virus: the NV gene is
848 required for pathogenicity. Mar Biotechnol (NY) 13, 672-683.

849 54. Holland, J.J., Peterson, J.A., 1964. Nucleic Acid and Protein Synthesis during Poliovirus
850 Infection of Human Cells. J Mol Biol 8, 556-575.

851 55. Wertz, G.W., Youngner, J.S., 1970. Interferon production and inhibition of host synthesis in
852 cells infected with vesicular stomatitis virus. J Virol 6, 476-484.

853 56. Ferran, M.C., Lucas-Lenard, J.M., 1997. The vesicular stomatitis virus matrix protein inhibits
854 transcription from the human beta interferon promoter. J Virol 71, 371-377.

855 57. Ahmed, M., McKenzie, M.O., Puckett, S., Hojnacki, M., Poliquin, L., Lyles, D.S., 2003.

856 Ability of the matrix protein of vesicular stomatitis virus to suppress beta interferon gene
857 expression is genetically correlated with the inhibition of host RNA and protein synthesis. J
858 Virol 77, 4646-4657.
859 58. Clinton, G.M., Little, S.P., Hagen, F.S., Huang, A.S., 1978. The matrix (M) protein of vesicular
860 stomatitis virus regulates transcription. Cell 15, 1455-1462.
861 59. Dancho, B., McKenzie, M.O., Connor, J.H., Lyles, D.S., 2009. Vesicular stomatitis virus matrix
862 protein mutations that affect association with host membranes and viral nucleocapsids. J
863 Biol Chem 284, 4500-4509.
864 60. Mebatsion, T., Weiland, F., Conzelmann, K.K., 1999. Matrix protein of rabies virus is
865 responsible for the assembly and budding of bullet-shaped particles and interacts with the
866 transmembrane spike glycoprotein G. J Virol 73, 242-250.
867 61. Black, B.L., Rhodes, R.B., McKenzie, M., Lyles, D.S., 1993. The role of vesicular stomatitis
868 virus matrix protein in inhibition of host-directed gene expression is genetically separable
869 from its function in virus assembly. J Virol 67, 4814-4821.
870 62. Gaudier, M., Gaudin, Y., Knossow, M., 2002. Crystal structure of vesicular stomatitis virus
871 matrix protein. EMBO J 21, 2886-2892.
872 63. Graham, S.C., Assenberg, R., Delmas, O., Verma, A., Gholami, A., Talbi, C., Owens, R.J.,
873 Stuart, D.L., Grimes, J.M., Bourhy, H.,2008. Rhabdovirus matrix protein structures reveal a
874 novel mode of self-association. PLoS Pathogens, 4(12), e1000251.
875 64. Roy, A., Kucukural, A., Zhang, Y., 2010. I-TASSER: a unified platform for automated protein
876 structure and function prediction. Nature Protocols, 5, 725-738.
877 65. Glodowski, D. R., Petersen, J. M., Dahlberg, J. E., 2002. Complex nuclear localization signals
878 in the matrix protein of vesicular stomatitis virus. J Biol Chem 277, 46864–46870.
879 66. Ogden, J. R., Pal, R., and Wagner, R. R., 1986. Mapping regions of the matrix protein of
880 vesicular stomatitis virus which bind to ribonucleocapsids, liposomes and monoclonal
881 antibodies. J Virol 58, 860-868.

882 67. Connor, J. H. and Lyles, D. S. 2005. Inhibition of Host and Viral Translation during Vesicular
883 Stomatitis Virus Infection. J Biol Chem 280, 13512–13519.
884 68. Ammayappan, A., Lapatra, S.E., Vakharia, V.N., 2010. A vaccinia-virus-free reverse genetics
885 system for infectious hematopoietic necrosis virus. J Virol Methods 167, 132-139.
886 69. Lai, S.H., Jiang, G.B., Yao, J.H., Li, W., Han, B.J., Zhang, C., Zeng, C.C., Liu, Y.J., 2015.
887 Cytotoxic activity, DNA damage, cellular uptake, apoptosis and western blot analysis of
888 ruthenium(II) polypyridyl complex against human lung decarcinoma A549 cell. J Inorg
889 Biochem 152, 1-9.
890 70. Boyd, K.E., Wells, J., Gutman, J., Bartley, S.M., Farnham, P.J., 1998. c-Myc target gene
891 specificity is determined by a post-DNA binding mechanism. Proc Natl Acad Sci USA 95,
892 13887-13892.

893 **Figure Legends**

894 **Fig. 1. VHSV-IVb infection blocks IFN responsiveness. A)** EPC cells were left untreated or
895 treated with IFN (10 U/ml) and infected with VHSV-IVb (MOI = 0.1) at the different time points
896 indicated. Cytopathic effects (CPE) were assessed at 72 h.p.i. **B)** EPC cells were transfected with a
897 luciferase reporter driven by the IFITM1 promoter (IFITM1/luc) for 24 h followed by infection
898 with VHSV-IVb for 24 or 48 h, with or without EPC IFN treatment. Luciferase values were
899 quantified 6 h later and normalized to the uninfected, IFN treated control.

900

901 **Fig. 2. VHSV-IVb M inhibits host promoter activation. A)** EPC cells were co-transfected
902 with 0.4 µg IFITM1/luc construct, EPC-derived MAVS (0.3 µg) and plasmids encoding each of the
903 VHSV genes (0.05 or 0.1 µg), followed by luciferase assay 48 h later. Luciferase values were
904 normalized to IFITM1/luc + MAVS. Plasmid concentrations in all samples were equalized with
905 empty vector. **B)** EPC cells ($1X10^6$) were transfected with 2 µg of expression plasmids for the
906 indicated VHSV proteins expressed in frame with a C-terminal myc epitope tag. After 48 h, cell
907 lysates were separated by SDS PAGE and immunoblotted for protein expression with a myc mAb.

908 Note that VHSV M is less highly expressed because of its ability to inhibit its own expression from
909 the RNAP II-directed CMV promoter. **C)** EPC cells were co-transfected with IFITM1/luc (0.4 μg)
910 and various concentrations of a VHSV-IVb M expression plasmid (0.5-50 ng) for 24 h and then
911 treated with or without EPC IFN for 24 h followed by luciferase assay. Luciferase values were
912 normalized to IFITM1/luc + IFN. **D)** EPC cells were co-transfected with human IFN (hIFN)/luc
913 (0.4 μg), MAVS (0.3 μg) and various concentrations of a VHSV-IVb M expression plasmid (pCD-
914 M; 0.5-50 ng) for 24 h followed by luciferase assay. Luciferase values were normalized to IFN/luc
915 + MAVS. **E)** EPC cells were co-transfected with a SV40/luc construct (0.4 μg) and various
916 concentrations of pCD-M (0.5-50 ng) for 24 h followed by luciferase assay. Luciferase values were
917 normalized to SV40/luc alone.
918
919 **Fig. 3. VHSV-IVb M inhibits host mRNA expression. A)** EPC cells (1×10^6) were co-transfected
920 with or without a SV40/luc construct (0.8 μg) and various concentrations of a VHSV-IVb M
921 expression plasmid (0.1-0.5 μg) for 24 h, followed by RNA isolation. Luciferase mRNA levels
922 were measured by RT-qPCR. Data were normalized to β-actin mRNA levels. **B)** Tet-mSEAP were
923 co-transfected with or without IVb M (0.1 μg) into EPC cells for 24 h then treated with
924 doxycycline for 24 h followed by RNA isolation and RT-qPCR using mSEAP primer. For the
925 comparison indicated **** $p<0.001$.
926
927 **Fig. 4. VHSV M blocks nascent cellular RNA synthesis. A)** EPC cells were left untreated, treated
928 with 2 μg/ml α-Amanitin, 1 μg/ml Act. D or infected with VHSV-IVb (MOI = 1) for 24 h, then
929 cultured in 100 μM EU for 2 h. EU was visualized with Alexa594 via click chemistry reaction.
930 VHSV transfected cells were visualized using a polyclonal anti-VHSV antibody, followed by goat
931 anti-rabbit FITC secondary staining. **B)** EPC cells were co-transfected with 0.4 μg GFP and 0.1 μg
932 IVb M for 24 h then labeled with 100 μM EU for 2 h. EU was visualized with Alexa594 via click
933 chemistry reaction. **C)** EPC cells were transfected with SV40/luc, ITS1/luc or U6/Luc reporter

934 construct with 0.25 μg pCD-M/1×10^6 cells for 24 h followed by total RNA extraction and reverse
935 transcription to cDNA. Luciferase mRNA levels were quantified by RT-qPCR and normalized to
936 EPC β-actin mRNA levels. **D)** The data in C were expressed as a percentage of the control values
937 for each construct, demonstrating that relative inhibition was similar for all.
938
939 **Fig. 5. VHSV IVb M Localizes to the Nucleus and Cytoplasm and alters host mRNA**
940 **dynamics. A)** Cells transiently transfected with pCD-M were fractionated into nuclear membrane
941 (NM), soluble nuclear (SN), mitochondrial (M) and cytoplasmic (C) fractions using differential
942 centrifugation. Lysates were run on a 15 % SDS-Page gel and transferred to PVDF. IVb M was
943 detected with 1:1000 Myc antibody (Cell signaling). **B)** EPC cells were transfected with pCD-M
944 for 24 h. Fixed/permeabilized cells were incubated with anti-Myc primary antibody and then Goat-
945 anti-Rabbit secondary antibody conjugated with FITC. Cells were counterstained with propidium
946 iodide (PI) and viewed using a confocal microscope (100X). **C)** EPC cells were left uninfected or
947 were infected with VHSV-IVb virus (MOI 1) for 24 h or treated with Leptomycin B (LMB) for 3 h.
948 After infection/treatment, the EPC cell pellets were spiked with 1X10^^{5} HEK 293 cells before
949 fractionation followed by RNA isolation and RT-qPCR. Total ß actin mRNA levels and nucleus to
950 cytoplasm ratio of fish actin mRNA (**D**) were calculated. ß actin values were normalized to human
951 GAPDH values to control for differences in isolation efficiency under conditions in which
952 nuclear/cytoplasmic levels of the human transcript were not altered by treatment. * $p<0.05$; **
953 $p<0.01$; *** $p<0.005$; **** $p<0.001$.
954
955 **Fig. 6. VHSV-IVb M blocks RNAP II recruitment and activation. A)** EPC cells were
956 transfected with a tet regulated SEAP plasmid and pCD-M for 24 h and were then left untreated or
957 were induced with 2 μg/ml doxycycline for 4 h. After crosslinking, chromatin was
958 immunoprecipitated with antibodies to IgG and RNAP II and analyzed by RT-qPCR using primers
959 specific for the minimal CMV promoter. RNAP II recruitment was normalized to IgG control. For

960 the comparisons indicated * $p<0.05$; ** $p<0.01$; *** $p<0.005$. **B)** EPC cells were infected with
961 VHSV-IVb virus (MOI=5) for 0-72 h. Cell lysates were separated by PAGE and immunoblots
962 probed with antibodies recognizing RNA polymerase II CTD repeat YSPTSPS (α-RNAPII-Ps2),
963 total RNAP II, β-actin and VHSV structural proteins, followed by HRP secondary antibodies and
964 chemiluminescent detection. The bottom panel shows just the M band from the VHSV
965 immunoblot.

966

967 **Fig. 7. Comparison of fish rhabdoviral M proteins. A)** M proteins from various VHSV strains
968 and substrains (-IVb: MI03GL; KRRV: isolate of -IVa strain from Japan; F1: Egtved isolate of -Ia
969 strain from Denmark; Bog: NA-5 isolate from Bogachiel River; EB: EB#7 isolate from Elliot
970 Bay;), and from IHNV, SVCV and SHRV were co-transfected with SV40/luc into EPC cells for 24
971 h, after which time luciferase assays were performed. B) Immunoblot analysis of transfected viral
972 M proteins (1.0 μg per 1×10^6 cells) in EPC lysates, detected using anti-myc monoclonal followed
973 by HRP goat anti-mouse antibodies and visualization using chemiluminescence. *IHNV M protein
974 was so effective at shutting down transcription (including its own) that subsequent studies with
975 higher protein amounts were required to detect its expression (data not shown). **C)** EPC cells were
976 left untreated or transfected 0.1 μg VHSV-IVb M or VHSV-Ia (F1) M expression plasmids for 24
977 h, then labeled with 100 μM EU for 2 h. EU was visualized with Alexa594 via Click-IT chemistry
978 reaction.

979

980 **Fig. 8. Impact of amino acid changes to VHSV-IVb M on transcriptional inhibitory function.**
981 **A)** EPC cells were co-transfected with wild type -IVb M or M mutants (D62A or D62A/E181A)
982 along with SV40/Luc for 24 h followed by luciferase assay. ** $p<0.01$; *** $p<0.005$. **B)** Schematic
983 of the M mutants tested in A. **C)** Immunofluorescent microscopy of cells transfected with WT or
984 mutant M expression plasmids. Cells expressing M were identified by staining with a α-Myc mAb
985 (green), and the level of active RNAPII in M expressing cells (white arrow) was qualitatively

986 assessed by counterstaining with an αRNAPII-Ps2 pAB (red). Phosphorylation of serine-2 of the
987 RNAPII CTD is a hallmark of an active, elongating RNAPII. All samples were counterstained with
988 DAPI. Images are representative of multiple myc-positive clones for each transfection.
989
990 **Fig. 9. Replication of wild type versus M D62A and M D62A/E181A mutant viruses.** Viral titer
991 from media harvested from cells infected at the indicated time points at an MOI = 0.1 (A) or MOI =
992 1.0 (B). Error bars reflect SEM. * $p < 0.05$; ** $p < 0.01$; *** $p < 0.001$ mutant virus results
993 compared to rWT at the same time point.
994
995 **Fig. 10. Inhibition of host responses by wild type versus M D62A and M D62A/E181A mutant**
996 **viruses. A)** EPC cells were transfected with a SV40/luc for 6 h then infected with the indicated
997 viruses MOI = 0.1 or 1.0. Luciferase activity was quantified 24 h after infection and data
998 normalized by Bradford assay. Error bars reflect SEM. * $p < 0.05$; ** $p < 0.01$; *** $p < 0.001$
999 compared to rWT at the same MOI. **B)** Cells were left uninfected or were infected with the
1000 indicated virus then subjected immunostaining with either anti-VHSV antibody or anti-RNAP II
1001 phosphor-serine-2 antibody with DAPI counterstain. Note that column 1 (αVHSV) is from a
1002 parallel, identically treated culture as compared to the right two columns, and that the DAPI images
1003 correspond to the adjacent αRNAP II-Ps2 images. **C)** Quantification of the mean grey scale
1004 intensity found within the nucleus of virus-infected cells stained with the RNAP II phospho-serine-
1005 2 antibody. Error bars reflect SEM. *** $p < 0.001$ compared to uninfected controls. **D)** SRB assay
1006 was used to measure viability of EPC cells infected with rWT or mutant M viruses at 96 h post-
1007 infection at the indicated MOIs. Error bars reflect SEM. * $p < 0.05$; ** $p < 0.01$; *** $p < 0.001$
1008 mutant virus results compared to rWT results at the same MOI. **E)** EPC cells were infected with the
1009 indicated viruses at MOI = 0.1, and monolayers were overlayed with methylcellulose (0.75%). At
1010 48 or 96 h.p.i., cells were fixed with 10% formalin, stained with crystal violet, and imaged using
1011 phase contrast microscopy (bar = 100 μm).

1012

1013 **Fig. 11. Mutant M viruses elicit reduced transcriptional inhibition.** EPC cells were left
1014 untreated and unstained (A, D), untreated and stained (B, E) treated with Act.-D (C, F), or infected
1015 with the indicated viruses at a MOI = 1 for 24 h prior to EU labelling of nascent RNA (G–L). EU
1016 was conjugated to AlexaFluor-594 by Click-iT reaction and Flow data/IF images were collected.
1017 Images from coverslips placed in the cultures used for Flow were stained with αVHSV (green) post
1018 Click-iT reaction (red). Images correspond to the histogram directly above. The percentage of cells
1019 scored as AF-594 negative and AF594 positive are shown as an insert within each histogram.

1020

1021 **Fig. 12. Regulation of host IFN responses by wild type versus M D62A and M D62A/E181A**
1022 **mutant viruses. A)** Media collected at the indicated times post infection was used in an antiviral
1023 assay to assess the antiviral activity released, and quantified as antiviral units/mL (uIFN/mL) as
1024 discussed in the methods section. Error bars reflect SEM. * $p < 0.05$; ** $p < 0.01$; *** $p < 0.001$
1025 mutant virus results compared to rWT at same MOI. **B)** EPC cells were transfected with a Mx-1/luc
1026 reporter and then infected for 24 h with rWT or mutant viruses at MOI = 0.1 +/-, and then left
1027 untreated or treated with IFN for an additional 18 h. Luciferase activity was quantified and
1028 normalized to protein levels in cell lysates using a Bradford assay. **C)** EPC cells were transfected
1029 and treated as those in **(B)** but were infected with rWT or mutant viruses at an MOI = 1 before IFN
1030 treatment and luciferase activity quantification. Data are expressed as fold change of RLUs
1031 compared to the uninfected, untreated control. Error bars reflect SEM. * $p < 0.05$; ** $p < 0.01$; ***
1032 $p < 0.001$ mutant virus results are compared to rWT or in pairwise comparison indicated by solid
1033 horizontal bars above the samples of interest.

1034

1035 **Fig. 13. Regulation of innate immune genes by wild type versus M D62A and M D62A/E181A**
1036 **mutant viruses.** RT-qPCR results from RNA harvested at the indicated times post-infection (TPI)
1037 at an MOI = 0.1 (A-C) or MOI = 1 (D-F). Synthesized cDNAs were assessed for VHSV RNA (A,

1038 D), EPC type I IFN (B, E) and fish Mx-1 (C, F). Data were normalized to a spiked internal control
1039 as described in the methods section and presented as a fold change in expression relative to
1040 untreated controls. Error bars reflect SEM. * $p < 0.05$; ** $p < 0.01$; *** $p < 0.001$ mutant virus
1041 results compared to rWT at the same time point.

Fig. 1

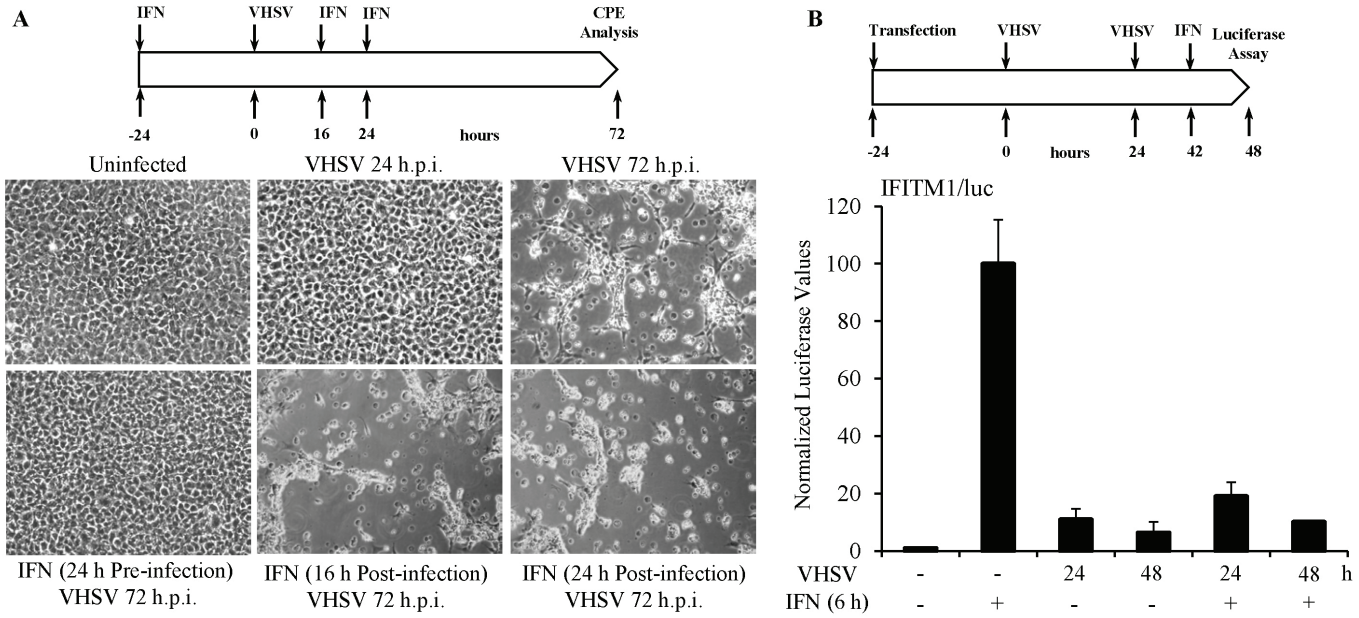

Fig. 2

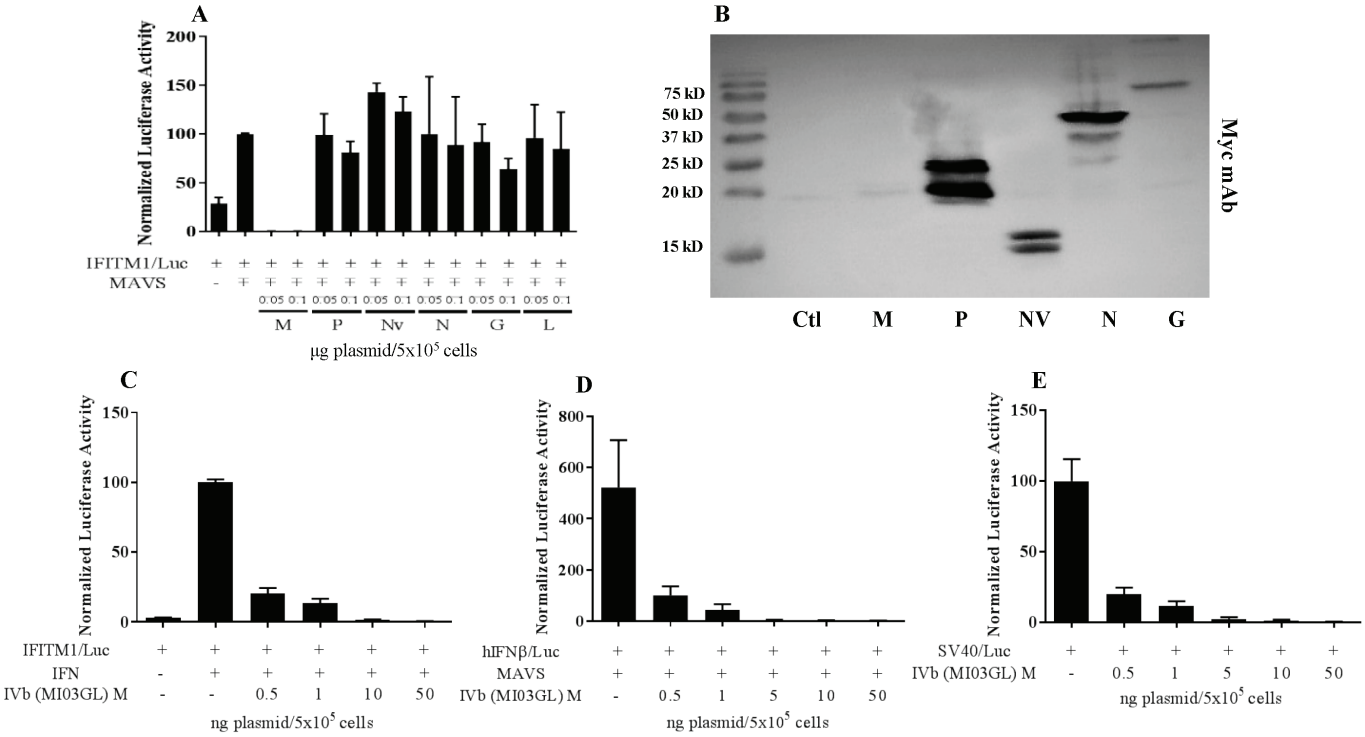

Fig. 3

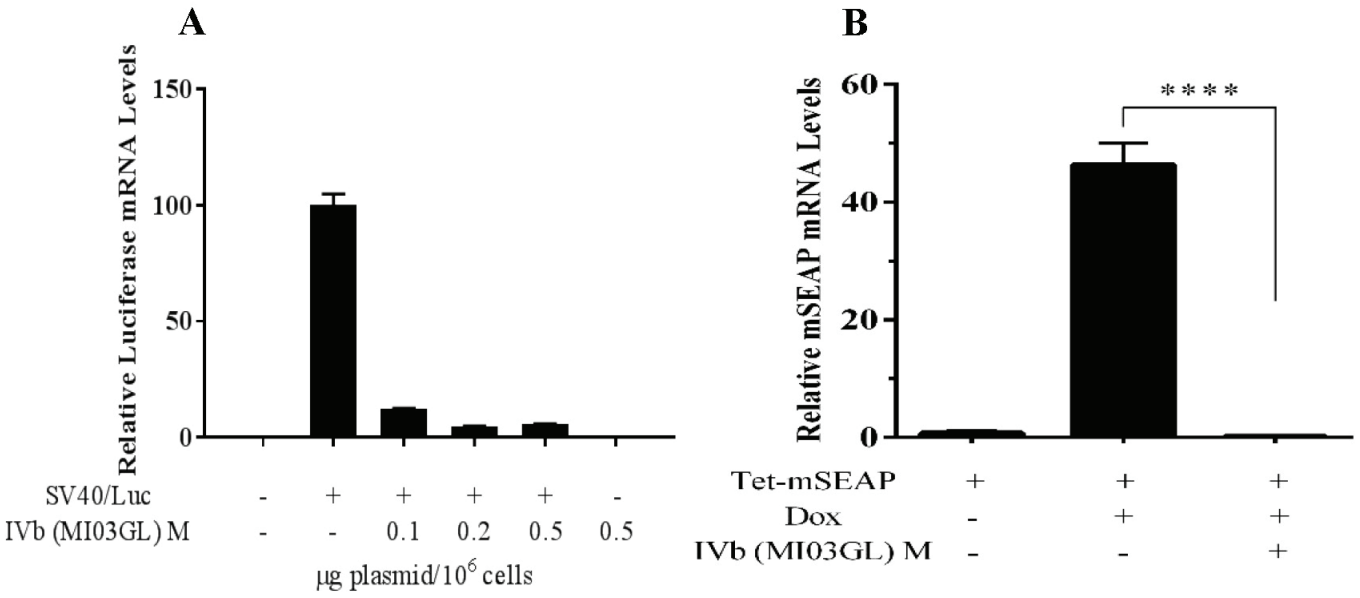

Fig. 4

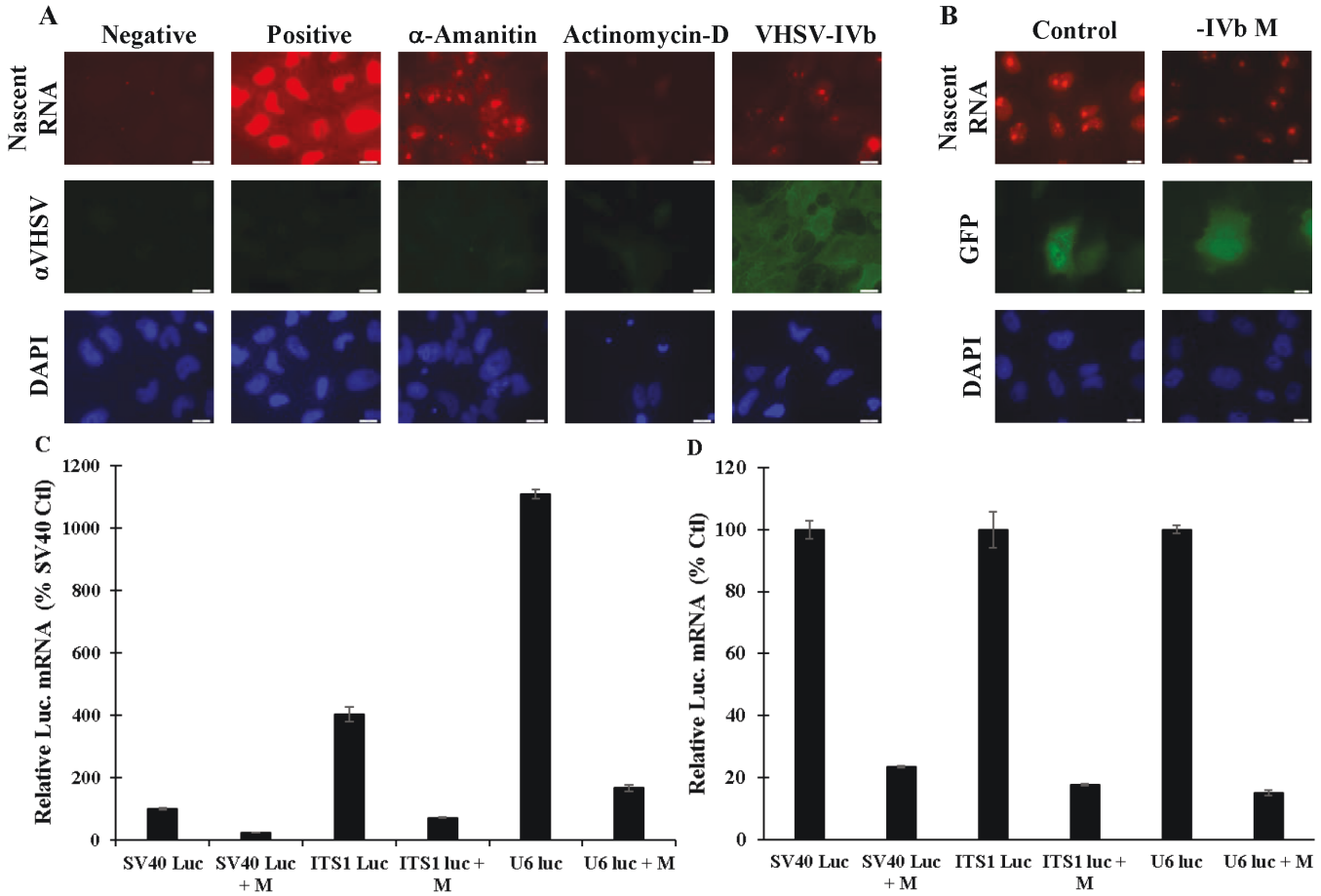

Fig. 5

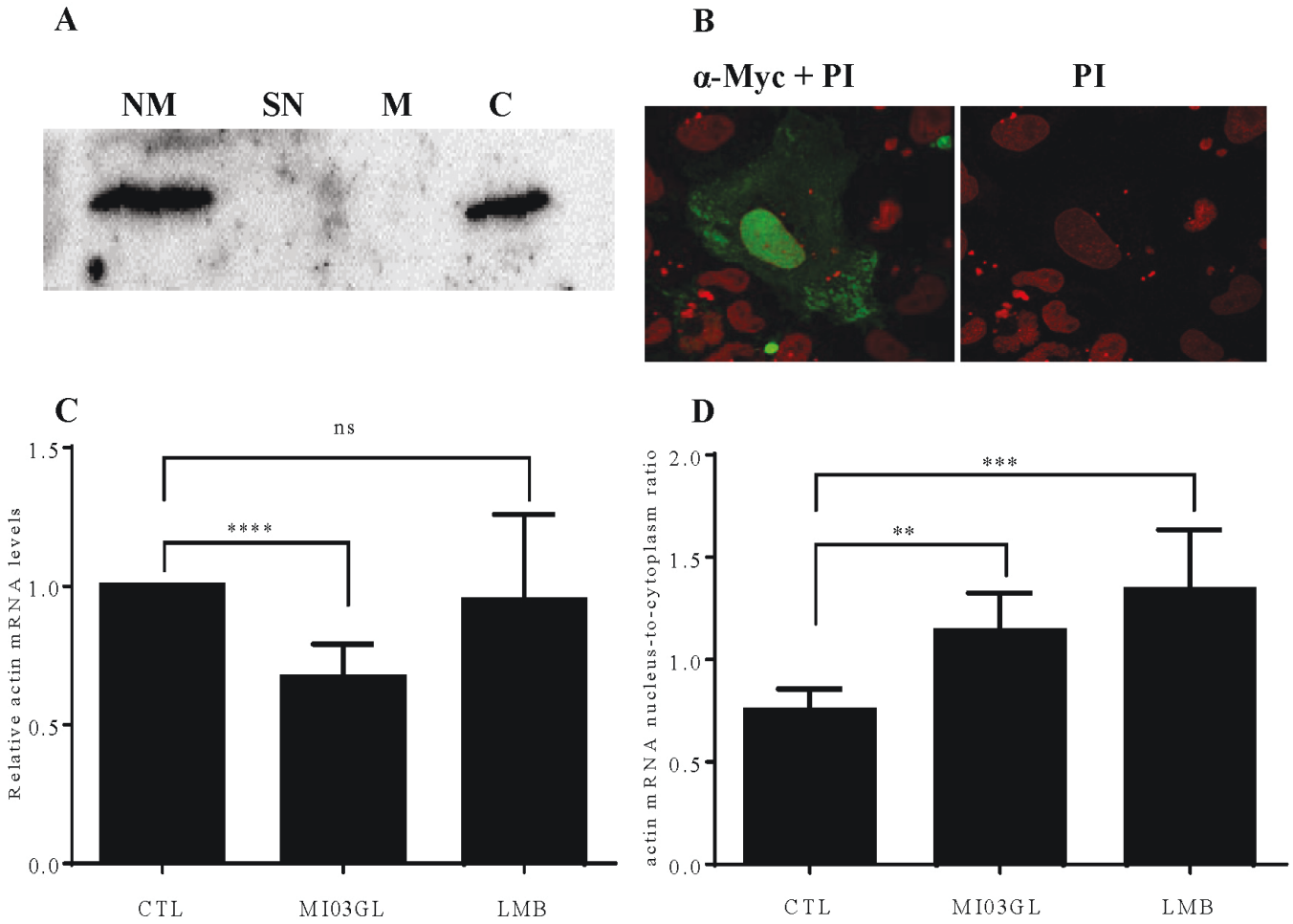

Fig. 6

A

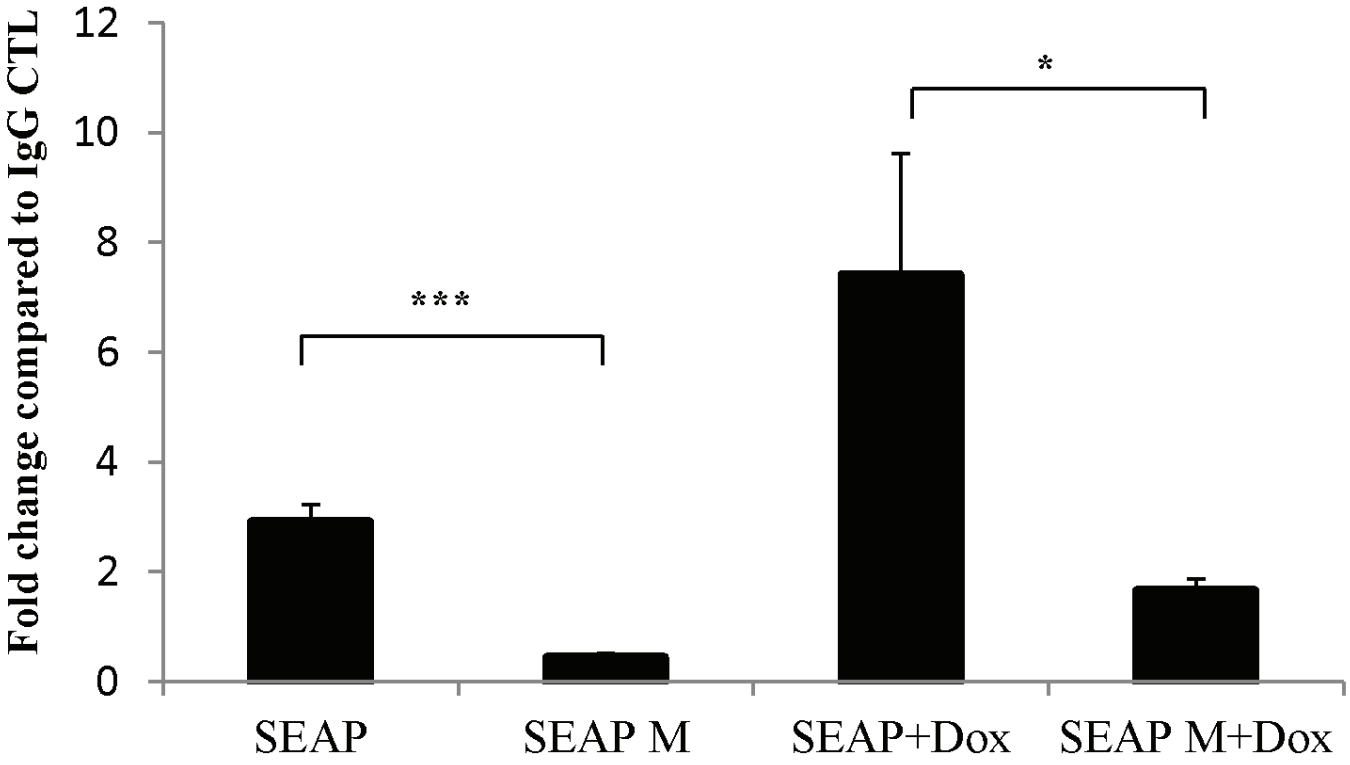

B

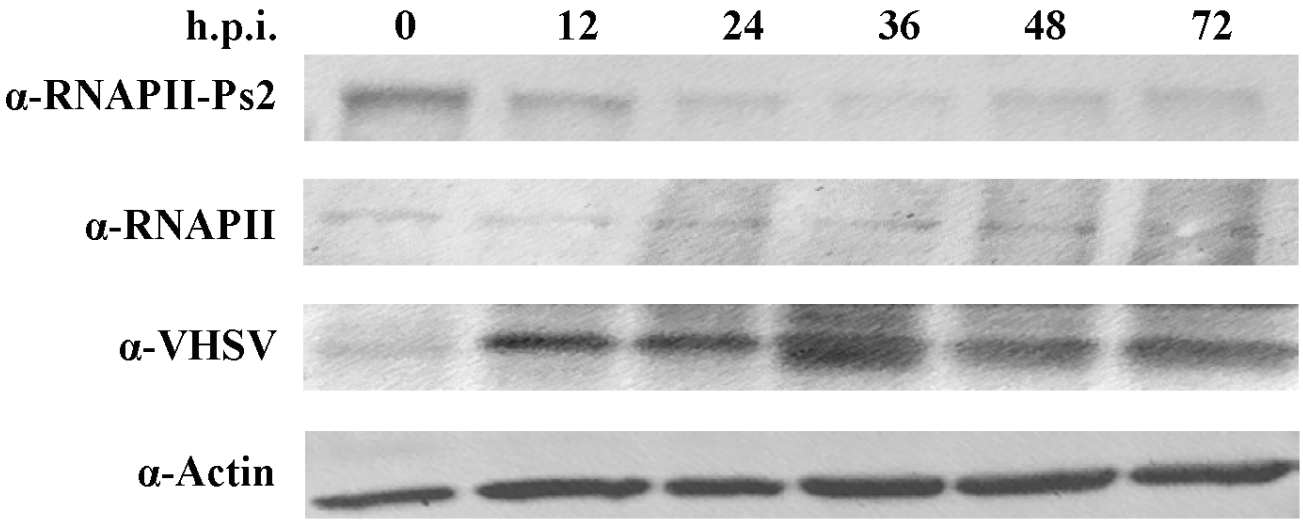

Fig. 7

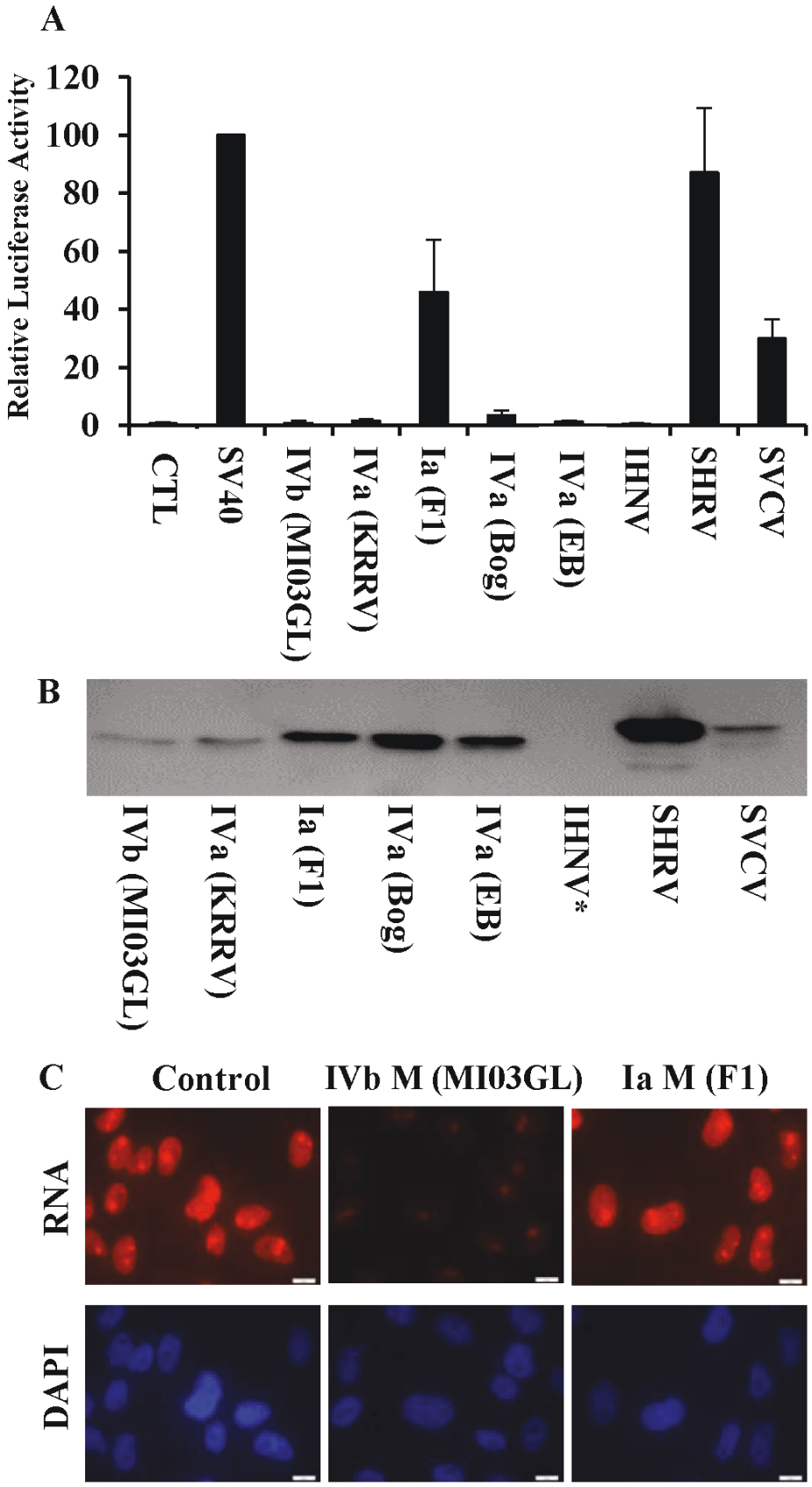

Fig. 8

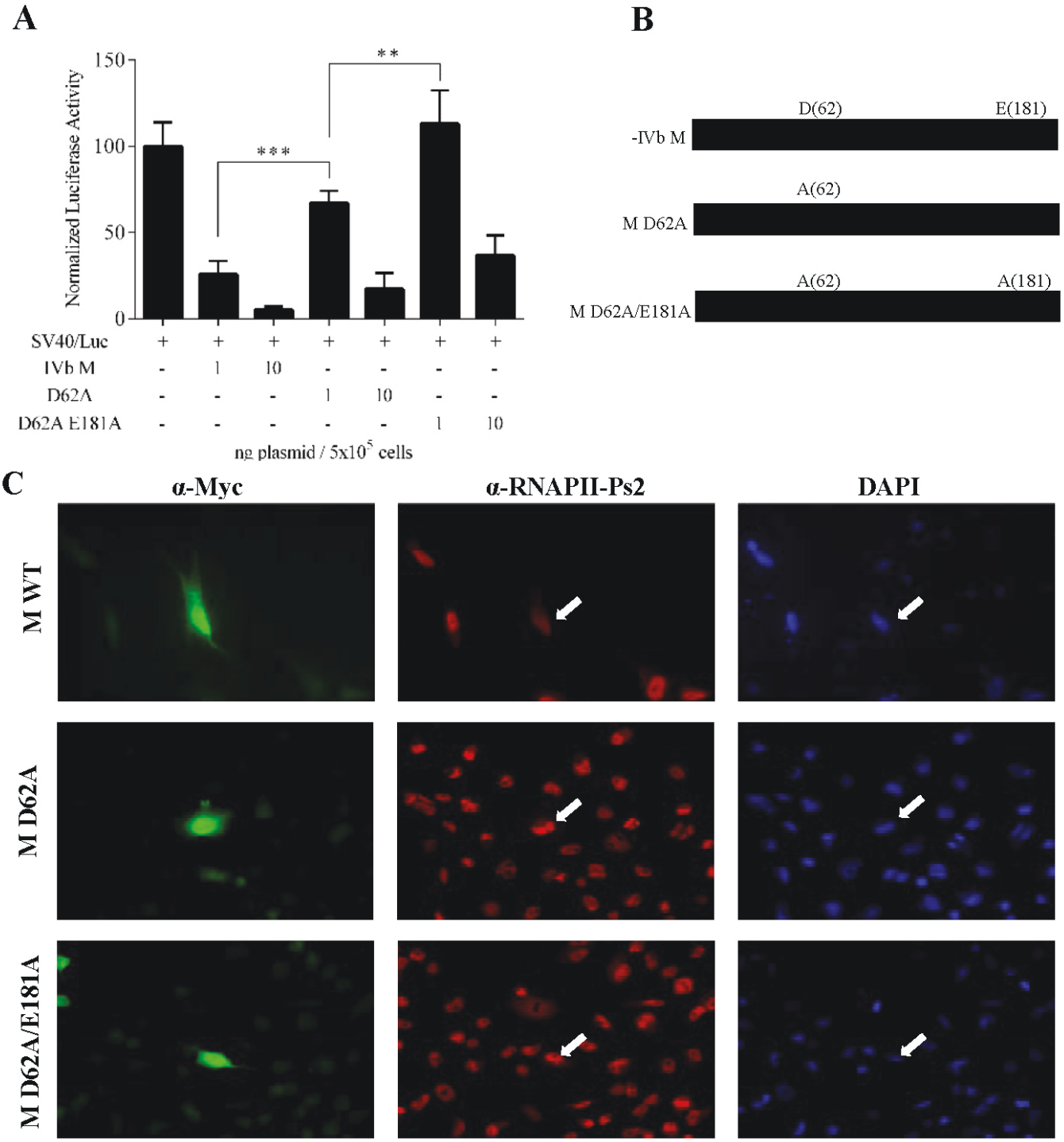

Fig. 9

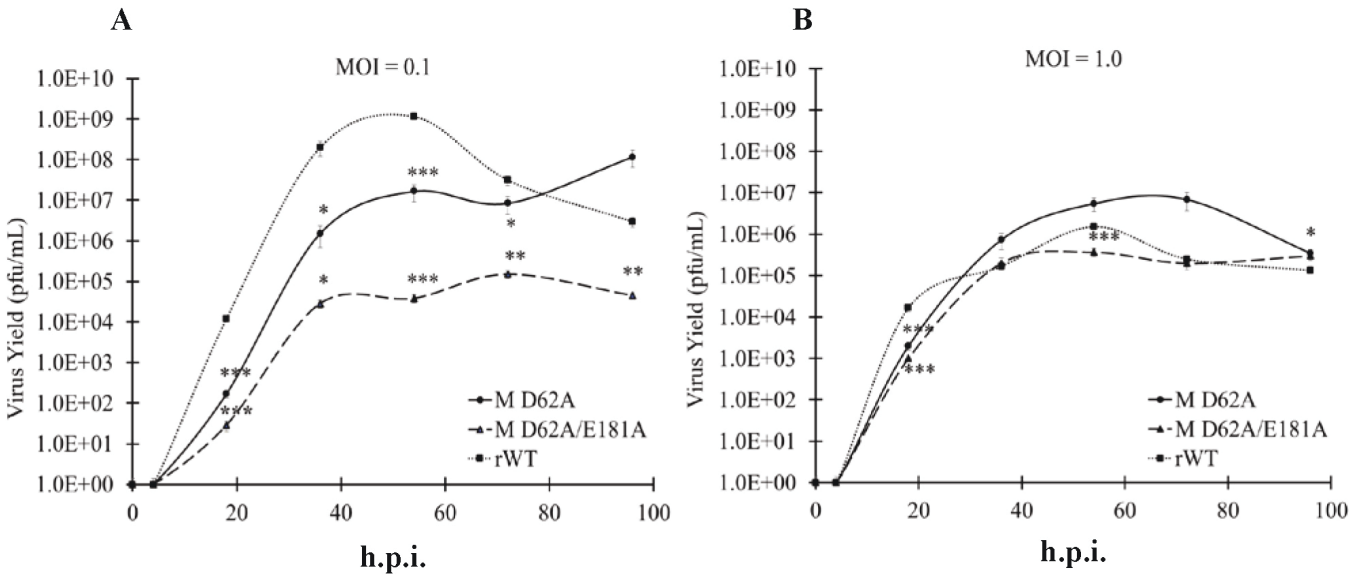

Fig. 10

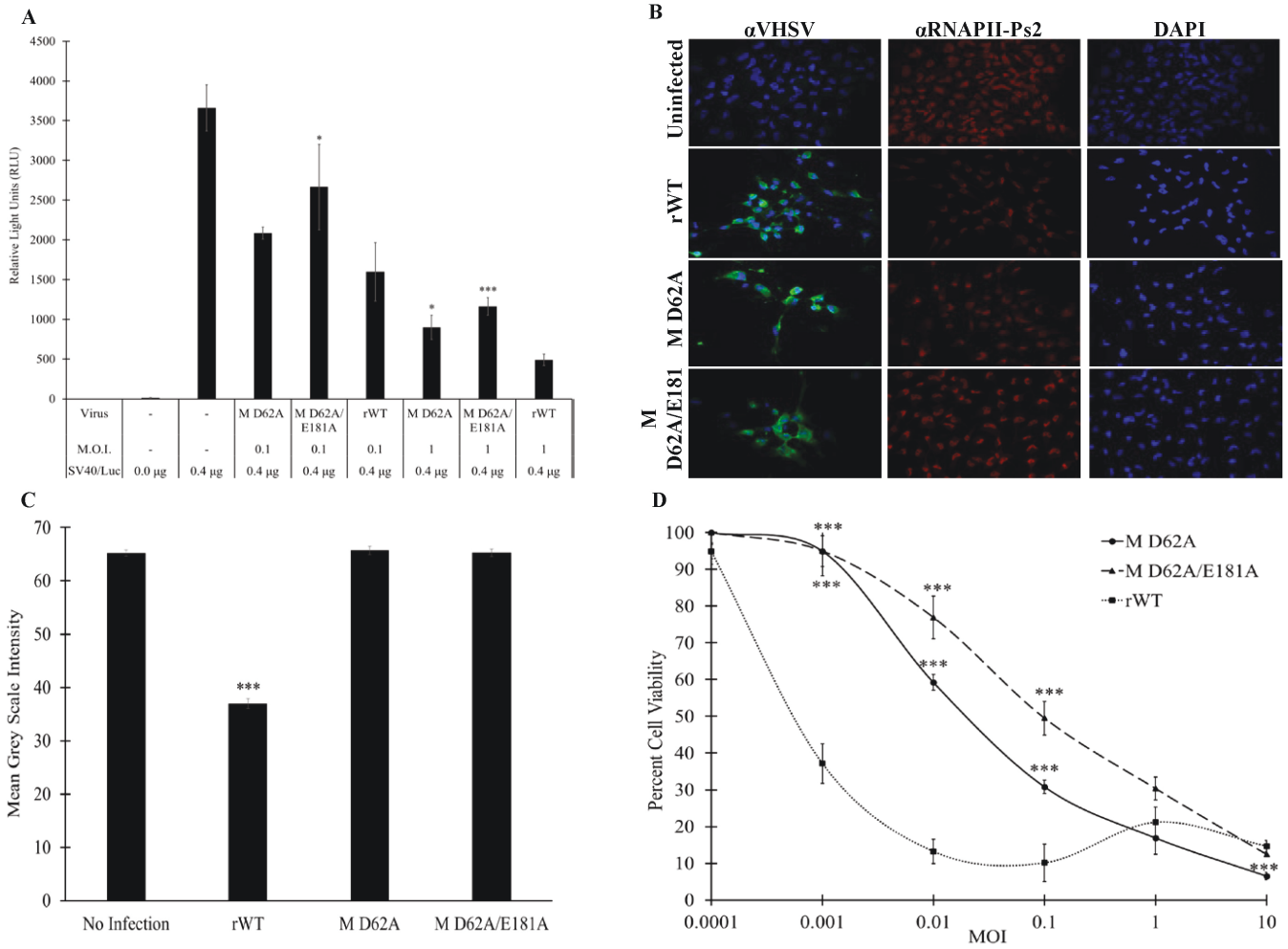

Fig. 10

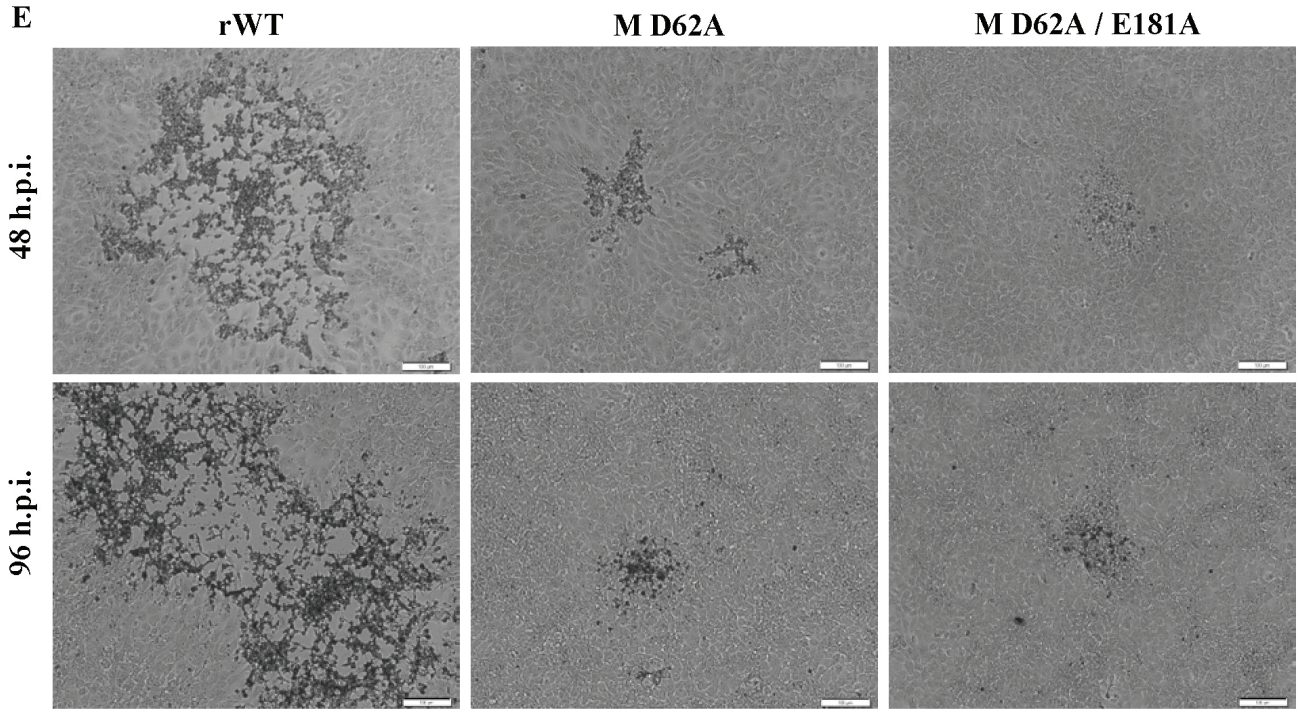

Fig. 11

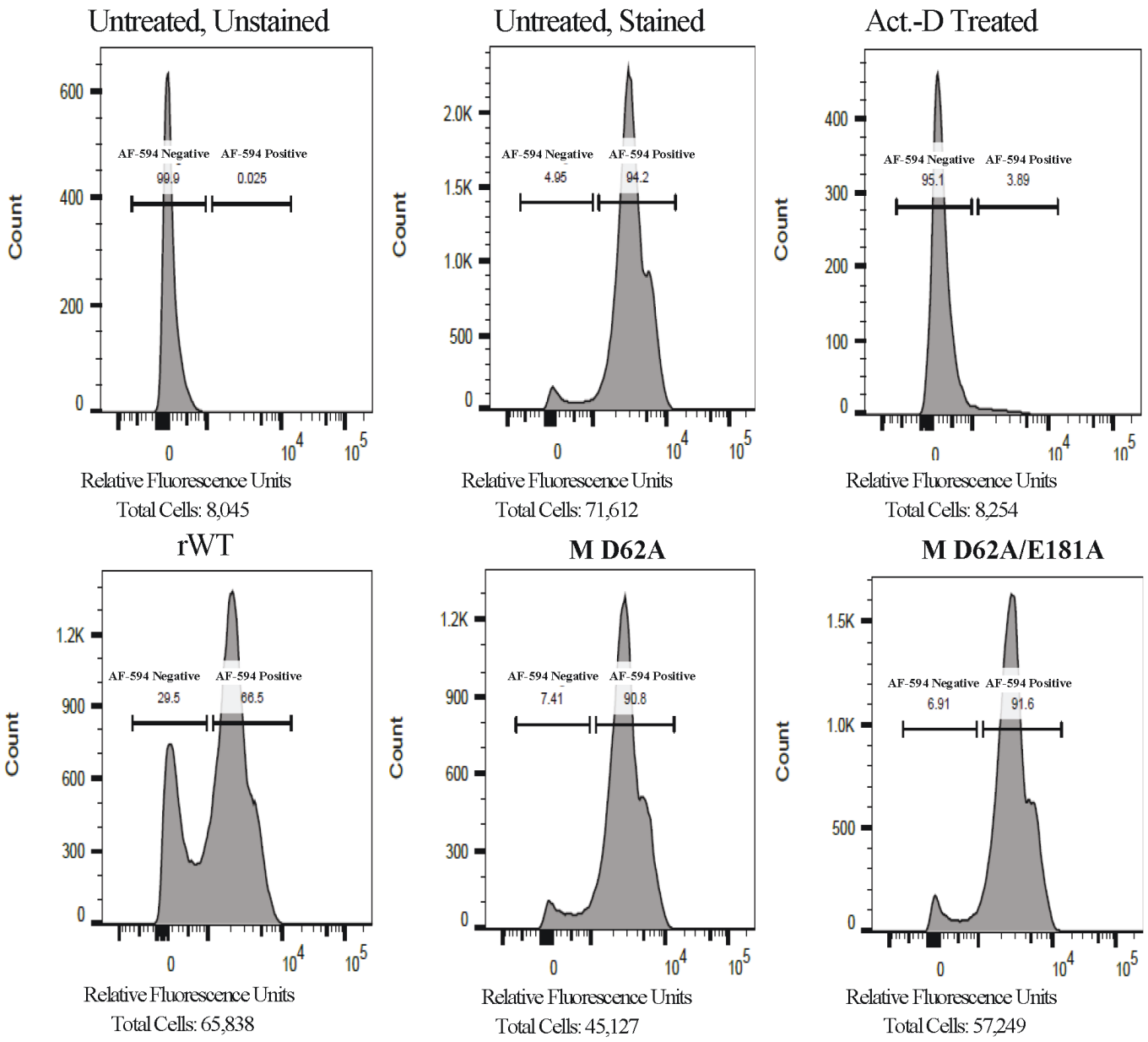

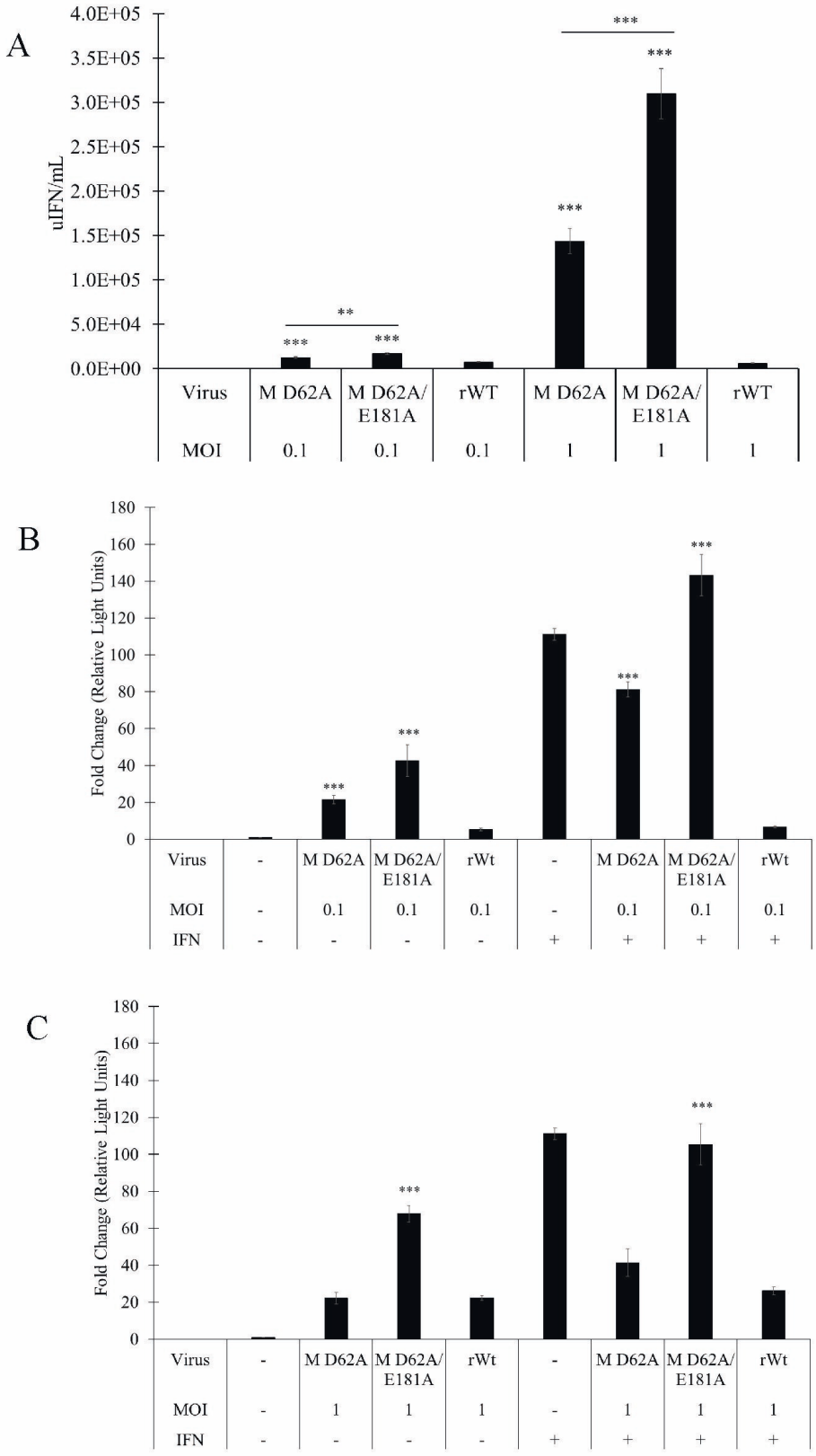

Fig. 12

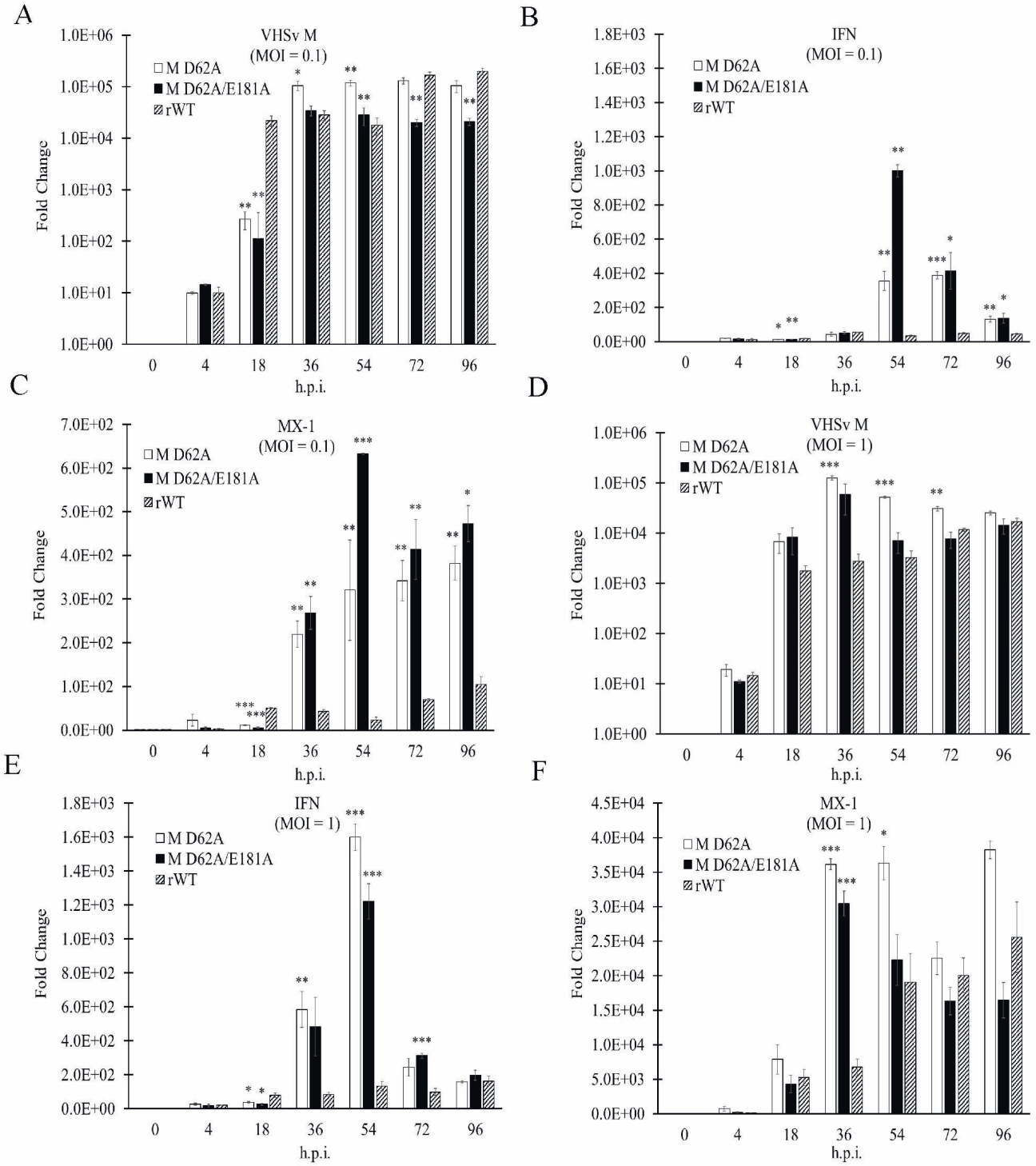

Fig. 13